Mechanisms of crustal growth in large igneous provinces: the North-Atlantic Province as a case study

Laurent Geoffroy*, Charles Aubourg,
Jean-Paul Callot and Jean-Alix Barrat

*Corresponding author: Laurent Geoffroy, Université du Maine, EA 3264, Ave O. Messiaen, 72085 Le Mans Cedex 9, France.
Email: laurent.geoffroy@univ-lemans.fr

Charles Aubourg, Université de Cergy-Pontoise, CNRS UMR 7072,
95031 Cergy-Pontoise Cedex France
Jean-Paul Callot, IFP, 1-4 avenue de Bois Préau, 92852 Rueil Malmaison Cedex France
Jean-Alix Barrat, Université de Bretagne Occidentale, IUEM, CNRS UMR 6538,
Technopole Brest-Iroise, 29280 Plouzané, France

Abstract

The mechanisms of magma crust accretion at LIPs are questioned using arguments based on the North-Atlantic case. Published and new data on the calculated flow vectors within dike swarms feeding the early traps and subsequent SDR-lavas suggest that most of the mafic magmas forming the North Atlantic LIP transited through a small number of igneous centers. The magma was injected centrifugally in dike swarms at some distance away from individual igneous centers along the trend of the maximum horizontal stress acting in the crust, feeding lava piles via dikes intersecting the ground surface. This mechanism is similar to that observed in present-day Iceland and, more generally, in mafic volcano-tectonic systems. The absence of generalized vertical magma transit in a LIP has major geodynamic consequences. We cannot link the surface extent of LIP magmas to the dimensions of the mantle melting zone as proposed in former plume head models. The distribution of LIP magmas at the surface is primarily controlled by the regional stress field acting within the upper crust, but is also affected by magma viscosity. The igneous centers feeding LIPs most likely represent the crustal expression of small-

scale convective cells of the buoyant mantle naturally located beneath the mechanical lithosphere.

1. INTRODUCTION

This contribution focuses on the localization of upper-mantle melting at the origin of Large Igneous Provinces (LIP). We need first to summarize the different views on LIP origin, which is a subject of great debate (see the website www.MantlePlumes.org).

Two distinctive stages of development are recognized in LIPs: the widespread emplacement of flood-basalts ('trap stage') and a (possible) consecutive 'volcanic-margin stage', during which syn-extension magmatism is concentrated along the break-up zone (e.g. White and McKenzie, 1989; Eldholm et al., 1995; Courtillot et al., 1999; Geoffroy, 2005). It is important to bear in mind the existence of these two developmental stages insofar as the geographic distribution and volumes of magma are different in each of them.

1.1. Trap stage

Traps or plateau basalts are flat-lying accumulations of mafic lavas that are emplaced during a relatively short time span. Some authors have used sedimentary records (White and Lovell, 1997) and wide-angle seismic surveys (Al-Kindi et al., 2003) to argue that magma underplating may also occur during this early stage. During trap emplacement, tectonic extension is usually small, and dilatation through dike injection seems to predominate over extension associated with normal faults (e.g. Doubre and Geoffroy, 2005).

Many authors have explained the large uplifted oceanic and/or continental areas covered with plateau basalts, as well as oceanic hot-spots located at the crest of broad seafloor swells, by the presence of more or less axisymmetric hot mantle plume heads beneath the lithosphere (e.g. Morgan, 1971; Courtney and White, 1986; Olson and Nam, 1986). White and McKenzie (1989) summarize the geological and geophysical features that are generally linked with postulated mantle plumes beneath the lithosphere. Mantle plumes are primarily thought to represent hot gravitational instabilities formed at the core-mantle boundary due to a core-mantle thermal boundary layer (e.g. Anderson, 2004). In parallel, the enriched trace-element

geochemistry of early traps at LIPs and oceanic islands basalts (OIB), as well as their rare gas isotopic ratios, is commonly explained by the postulated primitive composition of a lower mantle reservoir (e.g. Courtillot et al., 2003). Many models of plume head/lithosphere interaction have been discussed, such as: (1) sudden impact of a very hot plume (e.g. Richards et al., 1989), (2) progressive thermal erosion of the basal lithosphere by a long-lived incubating plume head (e.g. Kent et al., 1992), (3) interaction of a plume head with a lithosphere of variable thickness (e.g. White and McKenzie, 1989; Thompson and Gibson, 1989), (4) small-scale convection within the plume head (e.g. Fleitout and Froidevaux, 1986).

However, a range of new concepts and experiments has challenged the mantle plume theory (see extensive references in www.MantlePlumes.org). The reinterpretation of mantle seismic tomography raises questions about deep-seated mantle plumes, as exemplified by the Icelandic case (e.g. Foulger, 2002). The chemistry of early flood basalts and OIB could also be explained by melting of a much shallower compositionally heterogeneous mantle (e.g. Gallagher and Hawkesworth, 1992; Anderson, 1994). Notably, melting of eclogites (old subducted slabs) is proposed as a possible component in igneous provinces developed along ancient orogenic sutures (e.g. Foulger and Anderson, 2005). Hotter-than-normal mantle is also debated as a cause of LIP magmatism (e.g. Green et al., 1999). Different top-to-down processes have been proposed as an alternative to hot plumes, most of them invoking, although at quite different scales, upward counter-flow processes in the mantle due to the gravitational instability of cold lithospheric roots (e.g. King and Anderson, 1998; Lustrino, 2005).

1.2. VPM stage

Most volcanic passive margins (VPM, Fig. 1) are (1) consecutive to the emplacement of traps and (2) associated with anomalously thick oceanic crust following continental break-up. The main crustal characteristics of VPMs are listed in White et al. (1987), Eldholm et al. (1995), Bauer et al. (2000) and Geoffroy (2005), using data from both geophysical and geological surveys (Fig. 1). These margins are associated with significant magma accretion during lithosphere extension/rifting and subsequent break-up. Interestingly, the top-to-down trilogy of basalts, sheeted

complex and gabbros postulated for the VPM crust is strongly analogous with the structure of oceanic crust (Fig. 2). From the surface down to the Moho, the VPM crust (Fig. 1) is composed of (i) several wedges of seaward-dipping volcanic rocks (otherwise known as seismic 'SDR'), (ii) intensively intruded and stretched continental crust and (iii) large volumes of high P-wave velocity material usually interpreted as underplated high-Mg gabbros. SDR are made up of aerial or sub-aerial lavas, but also contain volcanic ejecta (e.g. hyaloclastites, tuffs, etc.). The tectonic significance of SDR has been discussed principally in Eldholm et al. (1995) and Geoffroy (2005). It is noteworthy that an inner SDR prism is usually located immediately above the stretched and intruded continental crust (e.g. Roberts, 1989; Planke et al., 2000; Geoffroy, 2005; Fig. 1).

For mantle-plume specialists, VPMs are thought to originate from continental break-up over the hot plume head or residual tail that remains after trap emplacement (e.g. White et al., 1987; White and McKenzie, 1989; Courtillot et al., 1999). However, small-scale convection due to the rifting process itself and/or pre-existing lateral variations in lithosphere thickness (e.g. Mutter et al., 1988; Keen and Boutilier, 1995; King and Anderson, 1998) could also account for the huge volumes of magma associated with VPMs without invoking any excess in mantle temperature. From numerical models of rapidly stretched continental lithosphere, Van Wijk et al. (2001) point out that the characteristic melt thickness of VPMs may be obtained solely through adiabatic melting of the sub-lithospheric buoyant mantle immediately before plate break-up. Anderson (1994 and 1995) proposed that the huge volumes produced at VPMs are the result of pull-apart processes over the fertile part of the mantle located beneath the mechanical lithosphere (called the "perisphere" or thermal boundary layer in the present paper). All these non-plume models assume that plate tectonics and plate geometry (craton edges) are sufficient by themselves to account for the origin of VPM and LIP as a whole.

1.3. Melting localization at LIPs

A fundamental aspect of LIP build-up concerns the localization of melting areas beneath or within the lithosphere. This problem has commonly been addressed through magma geochemistry. However, as outlined above, it is not always

straightforward to characterize the mantle reservoirs involved (i.e., lithospheric or asthenospheric mantle) because of the contamination of the melts by various crustal lithologies as illustrated by the Scottish Tertiary volcanics (e.g., Dickin et al., 1987, among others). Another approach to discuss the origin of the igneous activity is to establish the pattern of magma flow within the oceanic or continental crust. This was performed at the scale of a Proterozoic LIP by Ernst and Baragar (1992). From an AMS study in dikes, these authors argued that the McKenzie giant dike swarm (and related LIP) was fed centrifugally and horizontally in the continental crust from a central source (towards which the dikes converge) that was itself fed vertically from a mantle plume. In section 3.2, we return to the AMS methodology followed by these authors to infer the flow pattern in dikes. We should note that Phanerozoic LIPs are generally not associated with giant dikes (see section 2.3), and that no studies on the more recent LIP are specifically concerned with magma transfer from the mantle to the upper crust. Instead, in most LIP plume models, it is assumed either implicitly or explicitly that 'the extent of [flood basalts] gives a good indication of the area underlain by the mushroom head of hot mantle carried up by the plume' (White and McKenzie, 1989). The proposed diameters for melting plume heads could thus reach values of up to 2000 km (White and McKenzie, 1989; Hill et al., 1992).

The question of LIP feeding is also addressed by authors defending models that do not involve mantle plumes. Denying the existence of dike swarms that radiate from a single point, they propose that traps at LIPs are fed upward through regional dike swarms whose location is controlled solely by plate-related lithospheric stresses (e.g. Favela and Anderson, 1999; McHone et al., 2004) and not by a plume-related stress-field (i.e. radial due to a lithospheric swell, as in Ernst et al., 1995).

Thus, the most commonly held view for LIP formation involves a vertical transfer of magma from extensive zones of melting in the mantle to the upper crust (intrusions) or the Earth's surface (lavas, volcanic ejecta). This transfer is assumed to be direct (primary magmas) or indirect (magmas differentiated in crustal reservoirs). Inferring that the area covered by flood basalts corresponds more or less to the extent of mantle melting at depth is an important assumption since it determines the whole geodynamic model for the origin of LIP. In the present study, we make use of

the North Atlantic case to question this assumption by establishing the actual mechanisms of magma accretion during LIP growth.

2. THE NORTH ATLANTIC PROVINCE: WHAT KIND OF MAGMA FEEDING SYSTEM?

2.1. Volume estimates for the North Atlantic LIP

In the North Atlantic Volcanic Province (NAVP; Figs. 3 and 4), the earliest oceanic magnetoanomaly is dated as C24r, that is ca. -56/-54 Ma according to the Bergreen et al. (1995) time scale. The emplacement of Paleocene flood-basalts spanned about 6 Ma, from -62 to -57/-56 Ma (Hitchen and Richtie, 1993). Ar-Ar ages from the East-Greenland coastal dike swarm (Lenoir et al., 2003) indicate that the break-up is bracketed between 54 and 51 Ma, which is consistent with a sudden Eocene break-up event, coeval with the earliest oceanic accretion.

Coffin and Eldholm (1994) and Eldholm and Grue (1994) estimated the minimum volumes of magma in the NAVP (including initial traps and VPM) at no more than 6. 10^6 km^3, with rates of magma production reaching 2 km^3/yr. However, such an estimate is difficult to establish and should be considered only as a maximum value. For instance, most authors favoring the plume hypothesis unhesitatingly assume that W-Greenland, E-Greenland, the Faeroes and British Tertiary Igneous Province (BTIP) are parts of the same flood-basalt province (e.g. Saunders et al., 1997; Larsen et al., 1999). This shortcut hypothesis is debatable since there is no continuity of outcrop between W- and E- Greenland. Estimating the volume of underplated mafic magmas from the high-velocity zone (HVZ; Figs. 1 and 2) may also lead to unreliable results. Most authors agree that the HVZ represent substantial amounts of magma accreted (‘underplated’) at the Moho (e.g. Eldholm and Grue, 1994; Holbrook et al., 2001). However, Gernigon et al. (2004) have challenged the HVZ magma interpretation beneath the Voring Mesozoic basin. Should their observations be correct and applicable to other sedimentary basins, this would considerably decrease the estimated magma volume in the NAVP.

2.2. Igneous center distribution in the NAIP

An important characteristic of LIPs is the ubiquity of igneous centers punctuating the non-rifted and rifted continental/transitional crust. In the uppermost crust, igneous centers are represented by magma chambers and overlying hypo-volcanic intrusions, making up the roots of large polygenic volcanoes (e.g. Vann, 1978; Irvine et al., 1998; Chandrasekhar et al., 2002; Bauer et al., 2003). In the North Atlantic, these igneous centers are well known from direct observation and/or potential field data (Fig. 4). To a first approximation, the large sub-circular or elliptical magnetic and gravity anomalies associated with the igneous centers can be modeled by cylinder-shaped bodies of mafic to ultramafic rocks extending down to the Moho (e.g. Bott and Tuson, 1973; Bott and Tantrigoda, 1987).

The internal structure of these bodies is unknown. For instance, Bauer et al. (2003) proposed a crustal-scale interconnected network of mafic planar intrusions for the Messum igneous complex in Namibia. In the NAVP, at least 38 igneous centers were probably active during the trap stage (Fig. 4). Although not all igneous centers have yet been recognized and/or dated, their distribution appears to be (1) 2D in map view and (2) unrelated to the thickness of the crust (Fig. 4). According to Callot (2002), the spacing between offshore trap-stage igneous centers would vary from about 75±30 km in the Hatton area to 100±40 km in the Rockall-Faeroe Bank area (Fig. 4). This spacing decreases locally and significantly in the BTIP (35±3 km for the Sy-Mu-Am-Mu group (Callot, 2002). In this latter case, the distribution of igneous centers is evidently controlled by the location of the main Caledonian-inherited discontinuities which were reactivated during the Tertiary (Fig. 4B; e.g. Roberts, 1974).

Many igneous centers are also associated with the NAVP break-up process, so they are seen to punctuate the volcanic margins (e.g. Callot, 2002; Callot et al., 2002; Callot et al., 2004; Barton and White, 1997; Korenaga et al., 2000). Apart from the eroded along-strike exposures of the innermost parts of a VPM, as observed on the South-East Greenland coast (Figs 4 and 5; Myers, 1980; Bromann-Klausen and Larsen, 2002), the igneous centers associated with the break-up stage are less easy to distinguish physically due to their lower gravity and magnetic contrasts with the enclosing transitional or igneous crust (Fig. 5). However, the presence of relative

gravity highs (Fig. 5) and magnetic anomalies (Gac and Geoffroy, 2005) suggest that igneous centers in the VPM transitional crust display an aligned or zig-zag 1D pattern, or else a 2D arrangement within a narrow-band (Callot et al., 2002). Callot (2002) measured a 155±7 km spacing of igneous centers in onshore East-Greenland (area of low to moderate crustal thinning), decreasing to 58±12 km offshore where the lithospheric thinning was greatest (Fig. 5 and related caption). This latter value compares well with the wavelength of gravity and magnetic segmentation observed along the US East-Coast VPM at the continent-ocean transition (Behn and Lin, 2000).

It is noteworthy that, for at least two NAVP igneous centers (Rosemary Bank and Anton Dohrn; Fig. 4), the magmatic activity is likely to be Late Cretaceous in age (e.g. Jones et al., 1974; Hitchen and Richtie, 1993), thus predating the postulated Paleocene emplacement of the so-called Icelandic mantle plume. In addition, magmatic activity at igneous centers is often a persistent phenomenon. In some centers that were active during the trap emplacement, highly differentiated magma continued to be intruded during and even after the breakup process, sometimes at great distances from the volcanic margins (for example, the end-Eocene granites of the Mourne, Skye and Lundy igneous centers; Fig. 4) (Hitchen and Richtie, 1993; Saunders et al., 1997).

There is a general agreement that most LIP volcanism is of sub-aerial and fissural type. Low-viscosity tholeiitic or intermediate lava flows were fed by dikes intersecting the ground-surface as in present-day Hawaii, Afar or Icelandic volcanic systems (e.g. Self et al., 1997). Basaltic tuffs result from the dikes themselves (monogenic cones along fissures) or can be produced by ash eruptions from igneous centers related to polygenic volcanoes. It is thus evident that igneous centers and dike swarms play an essential role in distributing magmas within LIPs, not only at the ground surface (lavas and ejecta), but also within the intruded continental crust (magma crystallizing within the dikes themselves and in the igneous centers, hypovolcanic complexes and magma chambers).

2.3. Dike swarms and stress fields

In the NAVP continental domain, only a small number of offshore and onshore dike swarms have been identified from aeromagnetic surveys and direct observations, respectively (Fig. 3) (e.g. Larsen, 1978; Kirton and Donato, 1985; Speight et al., 1982; Myers et al., 1980; Bromann-Klausen and Larsen, 2002). In some offshore areas, high-resolution aeromagnetic data may however be missing or remain untreated. None of the recognized dike swarms correspond to giant dike swarms (i.e. swarms of dikes exceeding ca. 30 m in thickness): in the whole NAVP area, outcropping dikes (even through eroded basement) exhibit an average thickness rarely exceeding 2 m during the trap stage (e.g. Speight et al., 1982) and ranging from 3 m (highly stretched crust) to 8 m (weakly stretched crust) along the VPM (Bromann-Klausen and Larsen, 2002). Notable exceptions include individual intrusions such as the ~20-m-thick Cleveland Dyke (Scotland; McDonald et al., 1988) and the ~600-m-thick Kraemer Island dike-like intrusion (E-Greenland, Kangerlussuaq area).

Dike swarms trend parallel or sub-parallel to the maximum horizontal stress (e.g. Anderson, 1951), so the general pattern of the NAVP dike swarms may reflect the stress field in this area during the Paleogene (Figure 3A). However, this stress field was not uniform. A regional NW-SE-trending maximum stress during the Paleocene was associated with pre-breakup trap emplacement in the British Tertiary Igneous Province (e.g. Vann, 1978) and in the Faeroes area (Geoffroy et al., 1994; Fig. 3B). At the scale of the NAVP, the maximum horizontal stress was apparently radial and focused on the Kangerdlussuaq area, which contains outcrops of a large system of igneous intrusions (Fig. 3A). It should be noted that most of the observed dike swarms in the NAVP are centered on individual igneous centers (Fig. 3B). This is well established both in the trap area (e.g. Vann, 1978; Speight et al., 1982) and on the exposed parts of the VPM (Myers, 1981; Broman-Klausen and Larsen, 2002). In all studied cases, the finite horizontal magma dilatation associated with these swarms increases towards the igneous centers.

Therefore, in the NAVP (and generally in LIPs), magma transport in the brittle crust follows specific flow paths. The covering of vast continental areas by repetitive lava flows and volcanic products coming from a small number of fissure systems is not a hypothesis but a fact. The formation of dikes also plays a significant role in the

magmatic accretion of the transitional crust (Figs. 1 and 2). Although this mechanism is now well accepted, it still needs to be firmly integrated into a mantle/lithosphere model for Phanerozoic LIPs as the LIP magma feeding system is evidently connected with the distribution of mantle melting at depth. Some authors have proposed that dikes are fed vertically from mantle ridge structures (or linear thinned zones) which are undergoing partial melting and which follow the same trend as the swarms (e.g. Speight et al., 1982). Such a view is also implicit in the work of Al Kindi et al. (2003). Others such like White and McKenzie (1989) suggest that the magma migrates upward from a more or less homogeneously sub-circular melting mantle plume head (see a variation of this plume model by introducing pre-existing lithospheric thin spots in Thompson and Gibson, 1991 and Nielsen et al., 2002).

In the present study, we discuss these views using a statistical analysis of the flow vectors in selected dike swarms emplaced during both the trap- and SDR stages of NAVP evolution.

3. MEASURING FLOW VECTORS IN DIKES AND DIKE SWARMS

3.1. Magma flow vectors estimated by AMS

In the field, it is often difficult to determine with precision the fossilized flow vector in dikes. This is due to the scarcity of observable flow indicators both inside (e.g. oriented phenocrysts, elongated gas vesicles) and along the walls of the intrusions (e.g. mechanical lineations; Baer and Reches, 1987). Our method for studying magma flow in the NAVP dikes is based on the anisotropy of magnetic susceptibility (AMS). The AMS technique consists of determining of the maximum, intermediate and minimum principal axes (K1, K2, K3 respectively) of the magnetic susceptibility ellipsoid of a rock sample submitted to a weak magnetic field (for an explanation of the technique, see Rochette et al., 1991). The application of AMS to the petrofabric study of basaltic dikes has been extensively discussed (e.g. Ellwood, 1978; Knight and Walker, 1989; Hargraves et al., 1991; Rochette et al., 1991; Ernst and Baragar, 1992; Staudigel et al., 1992; Baer, 1995 ; Varga et al., 1998; Aubourg et al., 2002). Briefly, the magnetic foliation in basalts (i.e. the plane containing axis

K1 and K2, perpendicular to K3) is considered as reflecting the distribution of ferromagnetic oxides in the rock mass. Depending notably on the time of appearance of these grains during differentiation of the magma, their distribution is thought to correspond directly (e.g. Borradaile, 1988) or indirectly (Hargraves et al., 1991) to the fossilized magmatic foliation (i.e. a flow plane, see Nicolas, 1992). The AMS axis K1 (i.e., the magnetic lineation) is assumed by a number of authors to yield the orientation of the long axes of multidomain magnetic grains (i.e. Borradaile, 1988). In dikes, K1 would thus indicate the trend (but not the absolute direction) of the magma flow, that is, the magmatic lineation (e.g. Staudigel et al., 1992; Varga et al., 1998). The commonly observed obliquity of K1 axes relative to the walls of a dike was termed 'imbrication fabric' by Knight and Walker (1989). This imbrication has been used by some authors to determine the absolute direction of flow (e.g. Blanchard et al.,1979; Knight and Walker, 1989; Staudigel et al., 1992; Baer, 1995). This fabric would result from the downstream and oblique distribution of phenocrysts due to the strong velocity gradients existing in the magma near the walls of a dike (Fig. 6A).

3.2. Flow vectors determined solely from K3 axes

It is difficult to use the AMS technique in basaltic rocks because independent measurements of the magma flow direction from thin-sections in the (K1, K2) planes demonstrate that the K2 axis may also be sub-parallel to the alignment of phenocrysts in the rock mass (Ellwood, 1978; Moreira et al., 1999; Geoffroy et al., 2003; Callot and Geoffroy, 2004). This observation implies that K1 cannot be used indiscriminately as an indicator of the flow lineation in basaltic intrusions or lavas. In some cases, K1 would represent the intersection axis between shear-type and foliation-type magma planes (Callot and Guichet, 2003). Geoffroy et al. (2002) have proposed avoiding the incorrect use of K1 axes as a flow indicator by just considering the angle - when it can be distinguished - between magnetic *planes* with respect to each wall of the dikes (Fig. 6). In other words, we should use *solely the K3 axes* (poles of magnetic foliation) and the *poles of the dike walls* to determine a mean flow vector for the intrusion in order to avoid any misinterpretation of K1 or K2 as flow axes (Fig. 6). For example, Ernst and Baragar (1992) conclude there was a centrifugal flow of magma within the Proterozoic McKenzie giant dike swarm away from the area of convergence of the dike trends (and where they infer vertical flow).

While this is a major result, it is based solely on K1 statistics. Their data should be reworked using the above K3 methodology.

In addition, it may be appropriate to consider not just individual dikes but sets of parallel intrusions of similar thickness and composition, assumed (or demonstrated) to be of the same age (e.g. Callot et al., 2001). In such cases, the working hypothesis is that the set of intrusions were (1) emplaced at the same depth, (2) derived from the same reservoir and (3) governed by the same dynamics. We can then analyse the statistical grouping of the K3 axes from the whole-core data obtained from the two opposite walls of the dikes (which yield statistical imbrications at the walls), all data being represented in terms of 'dike coordinates' (see Rochette et al., 1991). We follow the same reasoning and computation to determine the mean flow orientation within the swarm as applied in the case of a single intrusion.

4. MAGMA FLOW DURING TRAP EMPLACEMENT STAGE: CASE OF THE ISLE OF SKYE

4.1. Dike swarms on the Isle of Skye

The Paleocene tholeiitic dike swarms of the BTIP follow a NW-SE to NNW-SSE trend and are related to Paleocene to Eocene igneous centers (e.g. Vann, 1978; Speight et al., 1982) (Figs. 3 and 7). Two sub-parallel sets of Paleocene dikes are known on the Isle of Skye (Mattey et al., 1977). Alkaline dikes seem uniformly distributed over the island and are associated with a small finite dilatation (not exceeding 1%). They probably fed the Skye Main Lava Series (Mattey et al., 1977). These dikes are postdated by a prominent tholeiitic swarm, focused on the Skye igneous center, that is associated with significant NE-SW trending magma dilatation (up to 20%) displaying a dual positive gradient (Fig. 7), not only towards the symmetry axis of the swarm but also towards the igneous center (Speight et al., 1982). According to Bell (1976) and Mattey et al. (1977), this major swarm fed the (nowadays, mostly eroded) tholeiitic traps ('Preshal Mohr lavas').

AMS studies have already been conducted in the Skye acid ring-dikes

(Geoffroy et al., 1997) and mafic cone-sheet (Herrero-Bervera et al., 2001). Both of these studies concluded that magma flow within the annular intrusions of the igneous center was probably sub-vertical and governed by bottom-to-top pressure gradients from a central crustal magma reservoir. Herrero-Bervera et al., (2001) also investigated the flow pattern within nine intrusions belonging to the regional dike swarm, concluding there had been some lateral magma flow within the mafic dikes. However, both their methodology and AMS interpretation were questioned by Aubourg and Geoffroy (2003).

4.2. AMS study of the tholeiitic swarm: technical approach

We present here, for the first time, a study carried out in 1995 on magma flow in the Isle of Skye dike swarm (Geoffroy and Aubourg, 1997). We sampled 522 samples in the walls of 30 basaltic dikes (1J to 30J). To avoid turbulent-flow, we cored dikes with a thickness not exceeding 1.65 m (average thickness: 0.9 m). We preferentially cored dike margins, where cooling had been more rapid, to obtain the largest flow velocity gradients and avoid post-injection re-arrangement of the flow-fabric. We selected only the basal 2.2 cm of the cores for measurement to minimize any effects due to weathering. The dikes were sampled from 6 sites (A to F in Fig. 7) located at different distances from the igneous center along the general NW-SE trend of the swarm. While all the dikes are tholeiitic, two of them (5J and 17J) nevertheless display high K_2O contents (> 1 wt%) (Table I). The tholeiitic dikes belong clearly to the Preshal Mohr type of basalts (Mattey et al., 1977; Kent and Fitton, 2000). The well-defined trends in Fig. 8 suggest a single parental melt composition, with magmatic processes dominated by crystal fractionation, possibly within the same reservoir. The magnetic susceptibilities range from 10^{-4} to 10^{-1} SI, which clearly indicates the predominance of magnetite in the rock mass. The rock magnetic fabric is dominantly planar, with an average magnetic foliation ratio exceeding the average magnetic lineation in 74 % of the dike walls. In most dikes, there is a closer clustering of the K3 axes (Table II) compared to the much more scattered K1 axes at both walls of the intrusions. Oriented thin-sections made from five key samples demonstrate that both K1 and K2 could represent the flow lineation (Geoffroy and Aubourg, 1997), which justifies our prudence in using solely the magnetic foliation to determine the flow-vector orientation.

Because extreme caution is needed in applying AMS to mafic rocks, we used a very critical approach to interpret our results (see details in the Table II caption). In our study, 24 dikes out of a total of 30 provided results that could be interpreted in terms of orientation of magnetic foliation relative to at least one of the dike walls (Table II and Fig. 7). However, there is frequently a large discrepancy between the flow vectors computed from walls on either side of a dike, at the worst yielding nearly opposite directions (Table II and Fig. 7). We were only able to determine consistent flow vectors (see Table II caption) for both of the walls in eight dikes (1J, 6J, 20J, 21J, 22J, 24J, 26J and 28J), while considering as (possibly) valid the single-wall data from 5J, 11J, 12J and 18J (Table II).

Figure 7 presents all the interpretable data at both walls of each dike at all the studied sites. Figure 9 presents a statistical analysis of K3 and K1 axes grouped by area: all data from the NW or SE of Skye are pooled (groups 1 and 2, respectively) with the exception of data from site Ardvasar (A). In Figure 9, K1 and K3 statistics are expressed in dike coordinates (Rochette et al., 1992; this means than all AMS data are rotated with the dike plane oriented vertically, assuming an arbitrary N-S trend).

4.3. Analysis and interpretation of results

We summarize the Skye data as follows (Table II; Figs. 7, 9 and 10). Analysis of the individual data reveals that, apart from dikes 1J and 21J, flow vectors are all downward-plunging on the Isle of Skye. South-east of the igneous center (sites A to D), the flow pattern is complex. The flow vector is oriented outward from the igneous center for two dikes (1J and 18J), while it is directed inward in three cases (5J, 6J and 12J) and downward in two others (11J and 20J). North-west from the igneous center, the flow vectors are plunging both downward and outward (24J, 26J, 28J), with the exception of the inward- and downward-plunging sample 22J (Figs. 7, 9, 10).

The statistical study of data for the area NW of the igneous center (Fig. 9, group 1) shows that (in dike coordinates) the magnetic foliation (K3) yields a very clear imbrication at the ‘eastern’ walls (Φ angle: -7° with respect to the ‘North’), but this becomes less well defined at the western walls (Φ angle: +4° with respect to the ‘North’). This indicates that the dominant flow in this area is lateral and directed towards the NW (see Fig. 6). A clear imbrication is also encountered SE of the

igneous center (Fig. 9, group. 2) at the eastern walls (Φ angle: +18° with respect to 'North' on the diagram), with the statistical foliation being parallel to the dike at the western walls (Φ angle: 0°). This indicates a general southeastward lateral magma flow, i.e. away from the igneous center. Finally, the statistical orientation of K3 at the dikes walls at the Ardvasar site (Fig. 7) is clouded by the co-existence of lateral magma flows directed (geographically) both towards the NW and the SE (two clear maxima observed for K3 at each wall, apart from the E-W trend on Fig. 9).

To summarize, the majority of flow vectors in basaltic dikes from Skye are sub-horizontal to downward plunging, which argues strongly in favor of lateral feeding from one or several high-level magma chambers (Fig. 10). The generalized northwestward and southeastward flows in areas NW and SE of the Skye igneous center, respectively, can be interpreted in terms of centrifugal lateral feeding of dikes (belonging to the major tholeiitic swarm) from a magma chamber located at the Skye igneous center (Fig. 10). As both NW-ward and SE-ward lateral flows are encountered south of Skye, we propose to interpret this result as indicating either (1) a double-feeding source or, (2), the existence of post-injection back-flow fabrics in these dikes, as reported elsewhere (Philpotts and Asher, 1994). According to the first hypothesis, and since the Skye regional swarm is connected to the Mull igneous center via a sigmoidal but continuous dilatation axis (Fig. 3B), the northwestward flows recorded on southern Skye could tentatively originate from the contemporaneous Mull igneous center. Alternatively, we could also invoke the existence of a small magma chamber south of Skye (see the high level of finite dilatation calculated from dikes south of Skye in Fig. 7).

More specifically, we should note that the steepest plunges of flow vectors are often observed on dikes with the shallowest dips (e.g. dike 11J). In addition, most dikes that yield opposite directions of flow from one wall to the other (i.e. "class-4" dikes, see Table II) also exhibit the shallowest dips (dikes 16J and 17J, for example). These particular cases could well be explained by a normal-shear transposition of the flow-related fabric during solidification of the magma. Also, some of the results from NW Skye (e.g. 27J and 28J) probably represent the effect of a lateral intrusive flow combined with a lateral Couette-type displacement, respectively sinistral and dextral, in excellent agreement with the NNW-SSE orientation of the maximum principal

horizontal stress during the Tertiary in this region (England, 1988; Geoffroy et al., 1993; see Fig. 3). Another interesting point is the clear downward plunge of many flow vectors at some distance from the proposed feeding center (Figs. 7 and 10). The occurrence of a downward flow component in individual dikes has already been suggested from the analysis of flow-markers (Baer and Reches, 1987) and petrofabrics (Shelley,1985; Aubourg et al., 2002). Northwest of the Skye igneous center, about 50 km away from the magma-chamber, our data suggest that the magma flow vector could have been systematically downward in most of the dike swarm at depths of probably less than 3 km below the Paleocene topographic surface. As magma is injected from chambers at a level of neutral buoyancy (Rhyan, 1987), such a pattern could reflect the increase in magma density due to cooling within dikes farther away from their feeder source. Decreasing both lateral pressure gradients and negative buoyancy of the magma with respect to its host-rock would promote convection of the magma within the dike fissure. Another hypothesis would involve inclined levels of neutral buoyancy away from the summit of the Skye polygenic volcano, but this seems to conflict with the strong plunges of flow vectors northwest of Skye.

5. MAGMA FLOWS AT VPM STAGE: EAST GREENLAND CASE

Between ~ 66°N and 68°N, the SE-Greenland coast partly exposes the western VPM that formed during the Eocene when Greenland and Europe split away to form the Reykjanes Basin (Figs. 3A and 5). Three field work campaigns in 1998, 1999 and 2000 were chiefly aimed at establishing the mean magma flows within a mafic dike swarm that crosscuts the transitional crust. This major dike swarm trends NE to NNE, with a clear dilatation gradient across-strike of the margin (NW to SE; Fig. 5). The gradient also increases towards the coastal igneous centers that punctuate the margin (Myers, 1980; Broman-Klausen and Larsen, 2002; Callot, 2002). The coastal outcrop area represents the flexed transitional crust located beneath an inner SDR wedge, which is nowadays eroded (Geoffroy, 2005). Many dikes were passively tilted during SDR formation. While some of them were injected during the flexing, another set of vertical intrusions post-dates the crustal flexing (e.g. Broman-Klausen and Larsen, 2002; Karson and Brooks, 1999; Lenoir et al., 2003).

We focused especially on the dike swarm centered on the Imlik-Kialineq igneous center (Fig. 5). This swarm is located at the SW-edge of the intrusive complex. A total of 44 dikes were sampled over a distance of 125 km, representing a total of 1172 drilling cores, making this analysis one of the most extensive ever carried out at the scale of a dike swarm. Based on a quantitative comparison between K1 and the observed textural fabric (i.e. paramagnetic phenocrysts) in thin sections from 52 cores, we concluded that neither K1 nor K2 could represent a valid estimate of the flow vector orientation (Geoffroy et al., 2003; Callot and Geoffroy, 2004). We thus drilled specifically chilled margins, considering only the imbricate foliation fabrics as reliable for inferring flow vectors.

The results of this study have already been published (Callot et al., 2001; Callot et al., 2004) and are only summarized here (Fig. 11):

1) Dike flow vectors could be interpreted for 24 out of the 44 studied intrusions (Fig. 11). In all cases but 2, the individual flow vector is directed to the SW;

2) Magma flow vectors at the scale of the studied dike swarm are remarkably consistent with a sub-horizontal magma flow towards the SW;

We thus have little doubt that the overlying SDR (volcanic formations) along this VPM were fed laterally (i.e. along-strike) from the upper-crustal igneous centers, and not vertically as initially thought.

6. MAGMA FEEDING MODEL FOR THE NORTH ATLANTIC LIP

6.1. The accretion center model

Thus, in the NAVP, we can infer that both traps and SDR are fed laterally by magmas collected in central crustal reservoirs. By itself, this result is not surprising (but needs to be confirmed), since this type of lateral feeding mechanism has long been established at slow-spreading or moderate-spreading oceanic accretion axes (e.g. Staudigel et al., 1992), in Iceland (e.g. Sigurdsson, 1987) or in Hawaii (e.g. Fiske and Jackson, 1972; Knight and Walker, 1988; Tilling and Dvorak, 1993; Parfitt

et al., 2002). Such a mechanism seems to be predominant in mafic volcano-tectonic systems (Parfitt et al., 2002). The lateral feeding model is also in good agreement with the general observation that lavas forming traps and SDR are differentiated by fractional crystallization in high-level crustal magma chambers (e.g. Cox, 1980; Andreasen et al., 2004). The mechanisms that control dike nucleation in magma chambers have been thoroughly investigated and do not need to be further discussed here (e.g. Mc Leod and Tait, 1999). Figure 12 presents a horizontal plan illustrating the concept of a single LIP 'accretion center' at the depth of the magma chamber. This accretion center model defines the elementary volcano-tectonic segmentation in LIP-related volcanic rifts and margins (Geoffroy, 2005; see also Ebinger and Casey, 2001). There is still some debate about the importance of lateral transport of low-viscosity magmas along cracks in controlling the regional distribution of traps and SDR. It is not easy to determine the along-strike length of individual dikes because dikes, like any tabular intrusion, are segmented in 3D. Nevertheless, magma has been shown to flow laterally as far as 100 km in the Hawaii dikes (e.g. Parfitt et al., 2002). We suggest above (Fig. 10) that some of the dikes on the Isle of Skye are fed by the Mull igneous center, corresponding to ~200 km of lateral flow (Fig. 3B). McDonald et al. (1988) concluded from geochemical evidence that the Cleveland dike (Fig. 3B) was fed laterally in a single pulse from the Mull igneous center, which would represent up to 430 km of sub-horizontal flow. Since low-viscosity lavas may flow over great distances from their eruptive fissures (Self et al., 1997; see also Fig. 12 for the role of faults), the above observations imply that the areal extent of LIP lavas is controlled by crustal processes rather than the mantle.

6.2. Could the whole of the North-Atlantic LIP magmas be drained through individual magma centers?

Igneous centers are thus the key to understanding the distribution of melting in the mantle underlying LIPs. Although the approach is highly speculative, it is possible to estimate the volume of magma that has transited through individual North-Atlantic igneous centers. We estimate that a minimum of 38 igneous centers were active during the trap-stage in the North-Atlantic (Fig. 4). The number of igneous centers active during the Eocene break-up stage is presently unknown (see chapter 1). Basing our estimate solely on the trap-stage, we obtain a volume of 10^6 km^3, which

seems a very large upper-limit value for the magma extruded and intruded during the period from 62 to 58 Ma (Paleocene/Earliest Eocene) (see White and McKenzie, 1989; Eldholm and Grue, 1994). The average upper-limit output rate at an individual igneous center would thus be ~7 10^{-3} km^3/yr. This value could be compared with the volume of magma represented by a dike intrusion phase to estimate an average eruption rate. However, as explained further below, such an exercise may be meaningless.

One of the best documented cases is from Hawaii, which provides an output of 3.3 10^{-3} km^3 (Cervelli et al., 2002). A similar value (7.5 10^{-3} km^3) is obtained from GPS measurement in the Galapagos, following the 1995 Fernandina flank eruption (Jonsson et al., 1999). The former estimates relate to both thin (< 1 m) and non-feeder intrusions. Although in a different geodynamic context, the lateral dike intrusion event monitored in the Izu Islands during the year 2000 corresponds to an estimated magma volume of ~1 km^3 (Nishimura et al., 2001). The volume of the Cleveland dike (thickness ~20 m) appears to attain 85 km^3 according to McDonald et al. (1988). Self et al. (1997) report a volume of 1300 km^3 for a single lava flow in the Columbia River LIP, thus implicitly setting a lower-limit value for the associated feeder dike. With such a range of values (over six orders of magnitude), it is not possible to evaluate the average volume of magma coming from a single igneous center. However, to obtain a gross estimate of the dike intrusion frequency and related magma volumes, we can tentatively refer to the two most intensively investigated mafic central volcanoes, i.e. Kilauea in Hawaii (e.g. Tilling and Dvorak, 1993) and Krafla in Iceland (e.g. Sigurdsson, 1987; Hofton and Foulger, 1996), which are situated in intraplate and plate-boundary settings, respectively. In both cases, the magma supply at igneous centers seems highly dependent on the progressive build-up of stress within the surrounding crust, irrespective of whether these stresses are due to gravity (Hawaii) and/or plate tectonics (Iceland).

The most recent intrusive activity on Kilauea (since 1956) appears to fit with *at least* one dike intrusion every 4 years, with periods of much higher activity (see Tilling and Dvorak, 1993). In the case of Krafla, it seems that periods of quiescence lasting 100-150 yrs (periods of tectonic stress concentration) alternate with episodic faulting/diking events (the last one spanning 6 years from 1975), during which ~20

dikes were injected laterally (Sigurdsson, 1987) parallel to the trend of the maximum horizontal stress. We should note that, both in Hawaii and Iceland, the volume of magma intrusion in dikes during an intrusive/eruptive event largely exceeds the volume represented by magma chamber deflation. In this way, diking events reflect the continuous feeding of the upper-crustal reservoirs by the mantle. The total flow out the Krafla reservoir during the last period of activity was ~ 1.08 km^3, which corresponds to an average of 8.10^{-3} km^3/yr over a period of 125 yrs. The mean output rate of Hawaii gives a strikingly similar value when averaged since 1840 (Tilling and Dvorak, 1993). These values compare well with the estimated maximum output rate of ~7 10^{-3} km^3/yr for an individual NAVP igneous center at trap-stage, suggesting that these igneous centers could be good candidates for the feeding of the whole LIP.

7. IMPLICATIONS FOR MANTLE MELTING

In the following, we discuss the implications of our results on mantle models. We use the term 'lithosphere' to refer to the mechanical entity, including the crust and part of the upper mantle, which is able to sustain stress over geological periods (e.g. Anderson, 1995). This lithosphere is thermally conductive. It is separated from the large-scale convecting mantle by a thermal boundary layer (TBL), in which temperature tends asymptotically to a convective-type gradient. This boundary layer is considered to be either stable or convective on the small scale (e.g. Jaupart and Mareschal, 1999; Morency et al., 2001).

Although other melting materials could be involved (see section 1), the adiabatic decompressive melting of rising mantle is generally acknowledged as the primary source of magmas at LIPs and oceanic ridges. In such cases, the area of mantle melting is evidently primarily controlled by the effective mantle temperature, pressure and volatile contents.

Our data suggest that no generalized vertical magma transfer occurs in LIPs (apart from beneath the crustal igneous centers themselves). This leads to major geodynamic consequences. The question we then need to address is the meaning of

igneous centers in relation to the pattern of mantle melting. With such a localized distribution of feeders for magma crust accretion in LIPs, how could the mantle be homogeneously melting (as in the initial plume head model)?

We should bear in mind that, at trap stage (see section 2-b), the distribution of igneous centers seems partly independent of the pre-magmatic rift zones in the North-Atlantic (Fig. 4). However, major discontinuities (e.g. Late Caledonian strike-slip faults, but also Mesozoic normal faults reactivating Caledonian thrusts) clearly have some influence on the igneous centers' distribution. During the VPM stage, this cannot be the case, because the igneous centers are regularly distributed within the necked and segmented crust (the area associated with SDR development, see Geoffroy, 2005; Fig. 5). In this latter context, their spacing seems related to the amount of lithosphere necking associated with the break-up (see section 2-b). At both stages of LIP evolution, the non-random distribution of igneous centers strongly suggests the existence of some kind of small-scale fluid instability within the lithosphere. The related "fluid-like" material could be present as melts (hypothesis 1: low-viscosity magma diapirs) or, as discussed further below, in the solid state (hypothesis 2: small-scale mantle diapirs).

7.1. Are magma diapirs possible?

Hypothesis (1) could be compatible with the following scenario: mafic to ultramafic magma rises homogeneously through the mantle lithosphere, collecting as a continuous sill-like layer(s) at the Moho, where it partially differentiates, and then ascends as diapirs to form igneous centers (Fig. 13A). It is likely that magma collects at levels of neutral buoyancy, thus explaining the presence of the HVZ at Moho depth under LIPs (Figs. 1 and 2; e.g. Fyfe, 1990; Holbrook et al., 2001). However, it is extremely improbable that Rayleigh-Taylor instabilities could develop in a basaltic layer (sill-like?) and, indeed, this should be ruled out. First, this would imply that the bulk density of the magma decreases more rapidly through fractional crystallization than the increase in density due to cooling. Second, the fluid behavior of a magma, whether of Newtonian or power-law type, depends on several factors including its temperature and crystal content (e.g. Weinberg and Podlachikov, 1995). A mafic magma extracted from a reservoir is more likely to behave as a Newtonian fluid, with a viscosity not exceeding 10^2 Pa.s (e.g. Spera, 1980). On the other hand, the lower-

crust viscosity, even in high heat-flow areas, is not expected to be lower than 10^{18} Pa.s. This constitutes a very strong obstacle for the development of Rayleigh-Taylor instabilities for a low-viscosity fluid. Nevertheless, some authors accept that a high-temperature diapir may decrease the host-rock viscosity at its edges (Spera, 1980; Rubbin, 1993). This phenomenon could be enhanced by partial fusion of the country rock. In addition, if the magma diapir behaves as a power-law fluid enclosed in a power-law 'ductile' crust, the buoyant stress of the diapir may also decrease the wall-rock viscosity (Weinberg and Podlachikov, 1995). However, whatever the true fluid behavior of the magma, the viscosity of the Q-rich lower crust would probably not fall beneath 10^{16} Pa.s (see for example Weinberg and Podlachivov, 1995). Such a high viscosity ratio between the magma and the host-rock suggests that this latter behaves elastically and would fracture (Rubbin, 1993). This may be related to the accepted geological observation that the emplacement of mafic plutons is always fracture-associated and never involves processes of magmatic intrusion (e.g. Shaw, 1980). Moreover, we note that even the existence of acid diapirs can be questioned (e.g. Clemens and Mawer, 1992). Finally, we should add that buoyant rising magma diapirs are expected to slow down, cool and finally solidify beneath the brittle-ductile transition in the crust. Such a scenario would be in complete contradiction with the postulated existence of large mafic magma chambers in the LIP upper crust.

We thus consider that the only plausible explanation for the distribution and role of LIP igneous centers as magma-feeders is that melting is focused within the TBL mantle itself (hypothesis 2). This may occur in two cases: (A) the TBL is a non-convective steady-state hot layer, but melt products or melting are however localized in specific areas, (B) the TBL exhibits small-scale 3D convection, and melting occurs specifically at the top of the uprising cells.

7.2. Steady-state TBL hypothesis

We first discuss the concept of a steady-state buoyant TBL with inhomogeneous melting.

Many authors have discussed the general issue of melt extraction and migration in an adiabatically flowing melting mantle, especially at spreading ridges (e.g. Spiegelman and Reynolds, 1999). Both magma percolation through a solid

compacting matrix and magma hydrofracturing have been investigated, with the latter mechanism being favored (e.g. Spera, 1980; Shaw, 1980; Nicolas, 1990). Most authors acknowledge that, overall, melt buoyancy contributes in a major way to magma flow in the mantle compared with compaction and dynamic pressures (e.g. Schmeling, 2000). Therefore, we do not expect large amounts of lateral magma flow within the mantle. However, provided the magma is extracted, a highly viscous dehydrated layer could be developed at the top of the melting zone that may act as a barrier channeling the magma flow from below (e.g. Morgan, 1987; Choblet and Parmentier, 2001). This led Madge et al. (1997) to explain along-axis variations in the thickness of igneous crust at slow-spreading ridges by the lateral upslope migration of melts. Such a process is assumed to occur at the top of large-scale undulations in a passive buoyant mantle, whose topology is inherited from the 3D lithosphere structure. In particular, areas with excess conductive cooling would act as melt deflectors. While this model contradicts the diapiric model of oceanic accretion proposed by Lin et al. (1990), it might be compatible with the existence of a regional and continuous low-resistivity layer in NE-Iceland, as shown from both MT and electrical measurements, with a minimum depth beneath the Krafla and Grimsvotn igneous centers (e.g. Bjornssön, 1985). This layer is interpreted as corresponding to a partially molten mantle (5 to 20% partial melt) at the roof of uprising asthenosphere domes. However, Madge et al.'s (1997) model can hardly be applied to the North-Atlantic continental lithosphere case, at least at the trap stage. Indeed, there appears to be no clear correlation at this stage between the thickness of basaltic products and the initial (Cretaceous, i.e. pre-magmatic) thermal state of the very heterogeneous lithosphere.

Melting instabilities could also develop laterally within a thermally destabilized sub-horizontal asthenosphere that is close to melting or partially molten. This scenario has been discussed by Tackley and Stevenson (1993) and Schmeling (2000), who investigated the lateral development of such instabilities using Newtonian and non-Newtonian viscosities, respectively. Although such instability propagation could explain the alignment of volcanoes with a progressive variation of ages, it cannot account for the observed 2D distribution of igneous centers of similar ages within the North Atlantic LIP (Fig. 4).

7.3. Convective destabilization of the TBL

We now explore the most plausible mechanism, i.e. partial melting of the TBL at the top of buoyant small-scale convection cells (Fig. 13). The spacing of igneous centers beneath the thinned NAVP lithosphere at the VPM is shorter than for igneous centers punctuating the thicker trap lithosphere, thus suggesting a relationship between igneous centers and mantle dynamics. The TBL is increasingly considered as undergoing natural small-scale convection, even in the absence of any additional heat supply (i.e. without invoking a mantle plume). This has been highlighted using different mantle rheologies and boundary conditions in a large number of experimental (e.g. Davaille and Jaupart, 1993; 1994) and numerical studies (e.g. Dumoulin et al., 1999; Morency et al., 2002; Korenaga and Jordan, 2002; Callot, 2002).

During the trap-stage, we should point out that the distribution of igneous centers is more or less homogeneous in 2D map view (Fig. 4), and not specifically associated with, for example, thinned Mesozoic crust. Therefore, at this stage, the upwelling of the melting mantle does not appear primarily dependent on previous tectonic stretching and thinning of the lithosphere. Such a conclusion has also been drawn from the time-evolution of igneous geochemistry in the BTIP (Thompson and Morrison, 1988; Kerr, 1994). These authors proposed a progressive and localized penetration of melting mantle into the continental lithosphere beneath the Skye and Mull igneous centers to explain the chemistry of the successive magma series.

To test the hypothesis that igneous centre spacing is correlated with small-scale 3D convection in the TBL, we would need to compare the characteristic wavelength λ of this small-scale convection with the average spacing of igneous centers in the North Atlantic (Callot, 2002). Theoretically, λ should be close to the thickness of the convective layer itself, since the convective cell aspect ratio generally lies between 1 and 1.35 (e.g. Houseman et al., 1981). Therefore, to resolve this issue, we need to evaluate the thickness of the convective TBL beneath a 60 My-old and relatively heterogeneous lithosphere. Although this thickness cannot be accessed directly, e.g. from geophysical data, it could be determined indirectly from experimental data. For example, Davaille and Jaupart (1993, 1994) propose an

equation where λ is inversely proportional to the surface heat-flux Qs (at the time of the convection). From the data of Morency et al. (2002), we can also derive different relations (depending on the type of mantle viscosity) between λ and Qm, the mantle heat flow beneath the conductive lithosphere.

Theoretically, we could also estimate (1), the crustal heat production (and its time-evolution, see Artemieva and Mooney, 2002), (2) the cooling and recovery of the continental lithosphere. These estimates could be used to correct present-day surface heat-flow in the NAVP (or lithosphere thickness) and correlate it with the past wavelengths of small-scale convection cells (Callot, 2002, unpublished PhD). The final step in testing the hypothesis would be to compare the theoretical wavelength with the actual spacing of igneous centers. While this point is not fully investigated here, we nevertheless give some first-order idea of the validity of small-scale convection at LIPs. It is clear that the above reasoning should be primarily applied for comparing trap areas that undergo little lithosphere thinning before the onset of trap formation. It is indeed difficult to estimate the true pre-magmatic lithosphere thickness if strong extension occurred (this depends notably on the rate of lateral cooling during extension). This should rule out any direct application to the NAVP because of its relatively complex Mesozoic evolution (e.g. Van Wijk and Cloething, 2002; Scheck-Wenderoth et al., 2006). However, according to the above argument, and as a first approximation, the thicker the present-day lithosphere (or the lower the surface heat-flux), the longer the average spacing between igneous centers. Callot (2002) tested this hypothesis on a range of trap areas worldwide (Deccan, Siberia, Parana-Etendeka, etc.) by making use of available geological, seismological and heat-flow data, but without correcting for the cooling and evolution of the lithosphere since the associated trap emplacement (however, we may consider that in many cases the error in thickness falls within the uncertainties of estimation of present-day lithosphere thickness).

Taking account of the evident serious limitations outlined above, Fig. 14 suggests a positive correlation between the lithosphere thickness (and indirectly TBL small-scale convection) and the spacing of igneous centers, even when considering the offshore Hebrides data (heterogeneous in thickness lithosphere). Note that the main discrepancy with the general correlation shown on Fig. 14 concerns the BTIP

igneous centers, where the close spacing is fault-controlled. It is noteworthy that many igneous centers lie along inherited lithospheric-scale or crustal-scale discontinuities (especially Late Caledonian sub-vertical shear-zones) (Fig. 4). At the same time, we should also take into account the existence of a transient Paleocene lithospheric stress field with the maximum horizontal stress converging towards a single point (Fig. 3). This could suggest a relationship during trap formation between a sudden change in regional-scale stress field and the enhancement of TBL destabilization, especially along the Caledonian discontinuities that were slightly reactivated during the Paleocene.

The distribution of igneous centers during the break-up stage seems much more focalized along the thinned and stretched Eocene VPM than at the trap-stage (Fig. 5). We note (Figs. 5 and 14) a strong decrease in the spacing of igneous centers (or postulated igneous centers from offshore gravity and magnetism) from the onshore internal margin (thicker crust and lithosphere) and the offshore/distal margin (thinnest crust/lithosphere with outer SDR). The data presented here strongly support a mechanism of VPM accretion similar to that at slow-spreading ridges, which partly explains the strong analogy in structure between the two crusts (Fig. 2). We point out that the wavelength of magma segmentation along the (offshore located) East Greenland VPM is very similar to that observed along the adjacent Reykjanes Ridge (Gac and Geoffroy, 2005). Similar observations have been made elsewhere (Behn and Lin, 2001). Some authors have proposed that magma may be focused at the top of small-scale convective cells, not only at slow-spreading ridges (Lin et al., 1990) but also at volcanic passive margins (e.g. Mutter et al., 1988; Keen and Boutilier, 1999). Holbrook et al. (2001) and Kelemen and Holbrook (1995) present arguments in favor of a strongly active upwelling mantle at VPMs, with active rates up to four times faster than passive rates (stretching-related). According to Huismans et al. (2001) as well as Van Wijk et al. (2001), a significant component of active mantle upwelling (and consecutive melting) may naturally occur beneath rifts at the end of passive stretching. However, Nielsen and Hopper (2002) argue for a slight temperature excess in the mantle. In any case, considering the true 3D architecture of a VPM, the active mantle upwelling should be regarded as small-scale 3D (channeled along the break-up zone) and certainly not 2D axisymmetric (see Geoffroy, 2005).

8. CONCLUSION

We show in this paper that magma distribution at the LIP ground surface has little to do with the extent of mantle melting at depth. At both stages of LIP evolution, the magma is channeled through pin-point crustal pathways that extend downward to localized melting zones in the mantle. We thus propose a magma feeding model for LIPs that is quite distinct from previous views of homogeneous mantle melting over plume heads (Fig. 15a) or homogeneous melting over deep “mantle ridges” (Fig. 15b). At both LIP stages, the best model describing the described pattern during traps emplacement invokes the existence of small-scale convection within the mantle (Fig. 15c). Small-scale convection in the TBL is not a specific LIP-related phenomena and may correspond to a generalized process beneath the mechanically rigid lithosphere (e.g. Morency et al., 2002; Korenaga and Jordan, 2002). It is probably a natural consequence of the negative buoyancy of the bottom of the lithosphere. However, such small-scale convection would have to be enhanced to explain the quite sudden mantle melting during the trap-stage in LIPs (and not elsewhere or at any other time). A transient excess in TBL temperature (e.g. plume head emplacement) could cause enhanced convection. We however suggest that other controls, such as a transient Paleocene compressive stress field (see Doubre and Geoffroy, 2003) acting in a lithosphere of highly variable thickness, could indirectly trigger mantle melting. This could be tentatively explained by diapiric destabilization at the top of the existing buoyant small-scale convecting cells, especially along reactivated lithospheric sutures. This latter explanation probably fits best with the available observations as well as the time and space constraints.

There is a strong structural analogy between VPMs and oceanic crust, which is based on their layering (Fig. 2), along-axis segmentation (Lin et al., 1990; Behn and Lin, 2000; Callot et al., 2002; Gac and Geoffroy, 2005) and crustal growth mechanisms (this study, for spreading ridges see Staudigel et al., 1992; Madge et al., 1992). This is probably due to similar mantle and crustal growth processes (Geoffroy, 2005). To improve our understanding of VPMs, we need to ask why some continental rifts function like oceanic rifts, although with enhanced magmatism (Fig. 2), while other rift systems do not. Both types of rift system (i.e. amagmatic and magmatic) are formed under extensional stress regimes, and may develop at the margins of cratonic

areas: the E-Greenland VPM is an example of a magmatic system, whereas the Baikal rift is an amagmatic system (e.g. Pavlenkova et al., 1992). This suggests that lithosphere edge effects (e.g. Anderson, 1994; Sheth, 1999) are not the sole indirect cause of magmatism at VPMs. We argued elsewhere that the pattern of lithospheric deformation at VPMs during break-up is closely dependent on the weakening of the upper lithosphere mantle by low-viscosity anomalies located within the mantle lithosphere (soft-point model of continental break-up; see, for example, Callot et al., 2002 and Geoffroy, 2005). These low-viscosity anomalies explain both the 3D strain localization and rift propagation at VPMs (Callot et al., 2002; Geoffroy, 2005). They fit very well with the postulated zones of mantle melting at depth presented here, thus giving a consistent model of combined magma, rheologic and tectonic evolution at VPMs (Geoffroy, 2005). Here again, the 3D sublithospheric convection pattern provides a key to understanding the origin and evolution of VPMs. Probably all rift systems are associated with small-scale convection in the TBL (see Korenaga and Jordan, 2002). The differences in along-strike segmentation between non-volcanic (e.g. Rhine Graben) and volcanic rifts (e.g. Ethiopian rift) suggest that the wavelength of small-scale convection is different in the two cases, thus also implying differences in mantle viscosity (see the discussion for the 3D pattern of oceanic accretion in Choblet and Parmentier, 2001). Our study does not provide a solution for this particular issue. We suggest however that during the latest stages of continental break-up in a LIP the small-scale convection turns suddenly from a poorly organized sub-lithospheric pattern (large wavelengths) to a more regular spreading-type regime (smaller wavelengths; see Fig. 14).

Acknowledgements. This paper is contribution n°2173 of the GDR Marges. The research was co-supported by Euromargin (LEC-01) and IPEV (Program 290). Don Anderson, Gillian Foulger, Donna Jurdy and Jolante Van Wijk are warmly thanked for their constructive and interesting comments. M. Carpenter is thanked for his efficient correction of the English language.

FIGURE CAPTIONS

Figure 1. Elements of a volcanic passive margin (from Geoffroy, 2005). Note the emplacement of traps before the syn-magmatic stretching and thinning of the continental crust.

Figure 2. Normal oceanic crust and VPM igneous crust: comparison of layering and P-wave seismic velocities. Data from Juteau and Maury (1999) and White et al. (1987).

Figure 3. A. The North Atlantic Volcanic Province during the C27-C25 trap-stage. 1: trend of the maximum horizontal stress inferred from dike swarms and fault tectonics (data from Geoffroy, 1994); 2: approximate distribution of Paleocene traps and sill swarms; 2: faults; 3: dike swarms. Note that the existence of Paleocene dikes along the SE Greenland coast is only hypothetical (see Lenoir et al., 2003). B. The British Tertiary Igneous Province, mainly after Speight et al. (1982). 1: traps: 2: igneous center; 3: dike swarms; 4: main crustal faults.

Figure 4. Recognized (red dots) or inferred (yellow dots) igneous centers in the North Atlantic Volcanic Province, not including those located at the continent-ocean transition (free-air gravity map; Smith and Sandwell, 1997). A24R is approximately located. This compilation is not exhaustive, since a number of new igneous centers probably remain to be discovered. The West-Erlend, Erlend and Brendan igneous centers (Smythe et al., 1983; Hitchen and Richtie, 1993), north of the Shetland Islands, lie outside the map area. Most igneous centers are recognized as Paleocene (also younger in some cases), with the possible exception of Rosemary Bank and Anton Dohrn, which are probably Maastrichtian (see Hitchen and Richtie, 1993 and references therein). Insert caption: AD: Anton Dohrn, Am: Ardnamurchan, An: Arran, Bs: Blackstone, Dn: Darwin, FB: Faeroe Bank, FC: Faeroe Channel, GB: George Blight bank, Gi: Geikie, HT: Hebrides Terrace, MC: Mourne-Carlingford, Mu: Mull, Rh: Rhum, RB: Rosemary Bank, RI: Rockall Island, Sr: Sigmundur, SK: St Kilda, Sy: Skye.

Figure 5. Geological map of E-Greenland. Location of exposed igneous centers and offshore gravity highs. After Esher and Pulvertaft (1995) modified.

Figure 6. The AMS 'magmatic foliation' method (Geoffroy et al., 2002). A: velocity fluid within a dike (Newtonian laminar flow) and related orientation of the imbricate magmatic foliation. The flow vector at each wall F is considered as being the axis, on the dike wall, perpendicular to the intersection axis Δ between the magnetic foliation and the wall. B. Example of flow vector determination in the case of horizontal (left) or sub-vertical (right) downward flow. All projections are lower-hemisphere.

Figure 7. Flow vectors calculated from the dike walls (see method in Fig. 6). Black stars and outward directed arrows: downward vectors; white stars and inward directed arrows: upward vectors. Iso-dilatation curves (in %) are calculated from the dike thicknesses (in Speight et al., 1982).

Figure 8. P_2O_5, TiO_2, and CaO contents plotted against FeO*/MgO. The contents are recalculated to 100 % on an H_2O-free basis. The fields for the Mull Plateau Group/Skye Main Lava Series (M1), Coire Gorm (M2), Central Mull Tholeiites/Preshal More (M3) basalt types are drawn using the analyses of dikes obtained by Kent and Fitton (2000).

Figure 9. Plot of the K3 and K1 axes (poles of magnetic foliation) from the western and eastern margins of the dikes in 'dike coordinates'. Group 1: E and F together; group 2: B, C and D. Ardvasar is A in Fig. 7.

Figure 10. Summary of flow-vector data and interpretation for the Isle of Skye.

Figure 11. Flow directions obtained for the East Greenland margin, on map and vertical cross-sections along-strike (in Callot and Geoffroy, 2004)

Figure 12. Concept of LIP accretion center, from Geoffroy (2005). Dikes inject from igneous centers in the trend of the maximum horizontal stress (σH). The figure illustrates the idea that tectonic stresses within the crust control indirectly the distribution of lavas. This control is two-fold: (1) magma erupts along dikes after lateral transport from the central magma reservoir; (2) the flow and distribution of lavas erupting from the feeder dikes is primarily controlled by their intrinsic viscosity but also, in many cases, by the footwall flexural topography of active normal faults that develop parallel to the dikes, following the trend of σH. This tectonic control of

lava flow takes place both during trap formation (e.g. Doubre and Geoffroy, 2003) as well as during the VPM break-up stage (SDR development). The SDR are analogous to fault-controlled roll-over structures that develop during the volcanic activity (Geoffroy, 2005).

Figure 13. Two interpretations of the relationship between TBL mantle and igneous centers. A: homogeneous melting and magma diapirism (ruled out in the discussion). B: small-scale convection model (favored)

Figure 14. Estimated thickness (in km) of the seismological lithosphere against igneous centers spacing. Data from LIPs (trap stage only) but also from several oceanic ridges (in km; in Callot, 2002).

Figure 15. Mantle models for trap provinces (plane view, outcrop area delimited by dashed line). Shaded: sub-lithospheric area associated with upward mantle flow and adiabatic melting. A. Plume head model. B. Mantle ridge model. C. Small-scale convection/diapirism model (favored).

Table I

Geochemistry of dikes from the Isle of Skye

Table II

Calculation of flow vectors carried out independently at each dike wall (as dikes trend mostly NW-SE to NNW-SSE, we refer to the dike wall facing the SW or NE as the W or E walls, respectively). We systematically used the imbrication angle ϕ between the local orientation of the wall and the mean minimum susceptibility (K3) axes to calculate the flow vector (see Fig. 6). The angular uncertainty on K3, with 95% confidence, is δK3. The following quality criteria were used. The fabric is thought to be interpretable when $\phi > 5°$. If $\phi \leq 5°$ (NO entry in the table), the result is considered questionable given the uncertainty on the orientation of the dike wall (±1° resolution using a Topochaix™ magnetic compass, due to irregularities on the dike wall, etc.). When $\delta K3 > \phi$ this corresponds to class 'A' results. In such cases, the imbrication angle is truly determined given the uncertainty on K3. When $\delta K3 \leq \phi$, this corresponds to class 'B' results. In such cases, there is an overlap between the K3

confidence area and the pole of the wall. The quality of the data at the scale of a dike depends on the consistency between the flow-vectors calculated at each wall. The angle γ between the two flow vectors defines the following sub-classes i in Table II: i=1 for $\gamma<30°$, i=2 for $30°\leq\gamma<60°$, i=3 for γ =60-90° and i=4 for $\gamma\geq90°$. Quality AB3 means that the W wall of a dike is of A quality, the E wall of B quality and that the angular separation between the W and E flow-vectors is comprised between 30° and 60°. We are only confident on the results from qualities AA1 to BB3, the latter type being the least reliable. We exclude any interpretation using data of quality i=4. We selected dikes for the final interpretation even if only one wall was determined, provided their quality was A (for example dike 18J where only the eastern wall provides flow). All detailed Skye data (individual core and averaged dike AMS and MS data) are available on simple request to the first or second author (laurent.geoffroy@univ-lemans.fr, aubourg@geol.u-cergy.fr).

REFERENCES

Al-Kindi, S., White, N., Sinha, M., England, R., Tiley, R., (2003), Crustal trace of a hot convective sheet, *Geology*, *31*, 207-210.

Anderson, E.M., (1951), *The dynamics of faulting and dyke formation with applications to Britain*, 206 pp., Oliver and Boyd, Edinburgh.

Anderson, D.L., (1994), The sublithospheric mantle as the source of continental flood basalts. The case against the continental lithosphere and plume head reservoir: *Earth and Planetary Science Letters*, *123*, 269-280.

Anderson, D. L., (1995), Lithosphere, asthenosphere and perisphere: *Review of Geophysics*, *33*, 125-149.

Anderson, D.L., (2004), What is a plume?, http://www.mantleplumes.org

Andreasen, R., D.W. Peate, C.K. Brooks (2004), Magma plumbing systems in large igneous provinces: Inferences from cyclical variations in Palaeogene East Greenland basalts, *Contribution in Mineralogy and Petrology*, *147*, 438-452.

Artemieva I.M., Mooney W.D., (2002), On the relation between cratonic lithosphere thickness, plate motions, and basal drag, *Tectonophysics, 358,* 211-231.

Aubourg, C., Giordano, G., Mattei, M., Speranza, F., (2002), Magma flow in sub-aqueous rhyolitic dikes inferred from magnetic fabric analysis (Ponza Island, W. Italy), *Physics and Chemistry of the Earth*, *27*, 1263-1272.

Aubourg, C, Geoffroy, L., (2003), Comment on paper: Magnetic fabric and inferred flow direction in dikes, conesheets and sill swarms, Isle of Skye, Scotland: *Journal of Volcanology and Geothermal Research*, 122, 143-144.

Baer, G., Reches, Z., (1987), Flow patterns of magma in dikes, Makhtesh Ramon, Israel*, Geology, 15*, 569-572.

Baer, G., (1995), Fracture propagation and magma flow in segmented dikes: Field evidence and fabric analyses, Makhtesh Ramon, Israel, *Physics and Chemistry of Dikes*, Baer and Heimann (Eds), 125-140 , Balkema, Rotterdam

Barton, A. J., White, R. S., (1997), Volcanism on the Rockall continental margin: *Journal of the Geological Society of London*, *154*, 531-536.

Bauer, K. Neben, K., S., Schreckenberger, S. Emmermann, B., Hinz, R., Fechner, K., Gohl, N., Schulze, K., Trumbull, R. B., Weber, K., (2000), Deep structure of the Namibia continental margin as derived from integrated geophysical studies, *Journal of Geophysical Research, 105*, 28829-28853.

Bell, J.D., (1976), The Tertiary intrusive complex on the Isle of Skye, *Proc. Geol. Ass., 87*, 247-271.

Berggren, W. A., Kent, D.V., Swisher, C.C., Aubry, M., (1995), A Revised Cenozoic Geochronology and Chronostratigraphy, *Geochronology, Time Scales and Global Stratigraphic Correlation*, edited by Berggren, W. A., Kent, D.V., Swisher, C.C., Aubry, M., Hardenbol, J., pp.129-212 , SEPM Special Publication No. 54.

Bjornssön, A., (1985), Dynamics of Crustal Rifting in NE Iceland, *Journal of Geophysical Research, 90*, 10151-10162.

Blanchard, J.P., Boyer, P., Gagny, C., (1979), Un nouveau critère de sens de mise en place dans une caisse filonienne: le 'pincement' des minéraux aux épontes: *Tectonophysics, 53*, 1-25.

Borradaile, G.H., (1988), Magnetic susceptibility, petrofabric and strain, *Tectonophysics,.156*, 1-20.

Bott, M.H.P., Tuson, J., (1973), Deep structure beneath the Tertiary Volcanic Regions of Skye, Mull and Ardnamurchan, North-west Scotland: *Nature, 242*, 114-116.

Bott, M.H.P. et Tantrigoda, A.D.A., (1987), Interpretation of the gravity and magnetic anomalies over the Mull tertiary intrusive complex, NW Scotland, *J. of the Geol. Soc. of London,144*, 17-28.

Bromann-Klausen, M., Larsen, H.C., (2002), East-Greenland coast-parallel dike swarm and its role in continental break-up, *Volcanic rifted Margins*, edited by M.A. Menzies, S.L. Klemperer, C.J. Ebinger, J.Baker, Eds., *362*, pp 133-158, GSA Special Paper.

Callot, J.P., Geoffroy, L., Aubourg, C., Pozzi, J.P., Mege, D., (2001), Magma flow direction of shallow dykes from the East Greenland margin inferred from magnetic fabric studies, *Tectonophysics, 335*, 313-329.

Callot, J.P., (2002), Origine, structure et développement des marges volcaniques: l'exemple du Groenland, Ph.D thesis, 584, Université Paris VI, France.

Callot, J.-P, Geoffroy, L., Brun, J.-P., (2002), 3D analogue modelling of volcanic passive margins, *Tectonics,. 21*.

Callot J. P., Guichet, X., (2003), Rock texture and magnetic lineation in dykes : a simple analytical model, *Tectonophysics, 306*, 207-222.

Callot, J.P., Geoffroy, L., (2004), Magma flow in the East Greenland dyke swarm inferred from study of anisotropy of magnetic susceptibility: magmatic growth of a volcanic margin, *Geophysical Journal International, 159*, p. 816-830.

Cervelli, P., Segall, P., Amelung, F., Garbeil, H., Meertens, C., Owen, S., Miklius, A., Lisowski, M., (2002), The 12 September 1999 Upper East Rift Zone dike intrusion at Kilauea Volcano, Hawaii, *J. Geophys. Res.,* 107, doi:10.1029/2001JB000602.

Chandrasekhar, D.V., Mishra, D.C., Poornachandra Rao, G.V.S., Mallikharjuna Rao, J., (2002), Gravity and magnetic signatures of volcanic plugs related to Deccan volcanism in Saurashtra, India and their physical and geochemical properties, *Earth and Planetary Science Letters, 201*, 277-292.

Clemens, J.D., Mawer, C.K., Granitic magma transport by fracture, *Tectonophysics, 204*, 339-360.

Coffin, M. F., Eldholm, O., (1994), Large igneous provinces: crustal structure, dimensions, and external consequences, *Review of Geophysics, 32*, 1-36.

Courtillot, V., Jaupart, C., Manighetti, I., Tapponnier, P., Besse, J., (1999), On causal links between flood basalts and continental break-up, *Earth and Planetary Science Letters, 166*, 177-195.

Courtillot, V., A. Davaile, J. Besse and J. Stock, (2003), Three distinct types of hotspots in the Earth's mantle, *Earth Planet. Sci. Lett.*, *205*, 295-308.

Courtney, R.C., White, R.S., (1986), Anomalous heat flow and geoid across the Cape Verde Rise; Evidence for dynamic support from a thermal plume in the mantle: *Geophysical Journal of the Royal Astronomy Society, 87*, 815-867.

Cox, K.G., (1980), A model for flood basalt volcanism: *Journal of Petrology, 21*, 629-650.

Davaille, A., Jaupart, C., (1993), Transient high Rayleigh number thermal convection with large viscosity variations, *Journal of Fluid Mechanics, 253*, 141-166.

Davaille, A., Jaupart, C., (1994), Onset of thermal convection in fluids with temperature-dependent viscosity: Application to the oceanic mantle, *Journal of Geophysical Research, 99,* 19853-19866.

Dickin A.P., Jones N.W., Thirlwall M.F., and Thompson R.N. (1987) A Ce/Nd isotope study of crustal contamination processes affecting Palaeocene magmas in Skye, *Northwest Scotland. Contrib. Mineral. Petrol. 96*, 455-464.

Doubre, C., Geoffroy, L., (2003), Rift-zone development around a plume-related magma centre on the Isle of Skye (Scotland): a model for stress inversions, *Terra Nova, 15*, 1-8.

Ebinger, C.J. and Casey, M., (2001), Continental break-up in magmatic provinces: An Ethiopian example, *Geology, 29*, 527-530.

Eldholm, O., Grue, K., (1999), North Atlantic volcanic margins: Dimensions and production rates, *Journal of Geophysical Research, 99*, p. 2955-2968.

Eldholm, O., Skogseid, J. Planke, S., Gladczenko, P., (1995), Volcanic margin concept, *Rifted Ocean-Continent Boundaries*, edited by Banda, E., pp. 1-16, Kluwer Academic Publishers.

Ellwood, B.B., (1978), Flow and emplacement direction determined from selected basaltic bodies using magnetic anisotropy measurements, *Earth and Planetary Science Letters, 41*, 254-264.

Esher, J.C. and Pulvertaft, T.C.R., (1995), Geological Map of Greenland, 1:2500000, *Geological Survey of Greenland* , Copenhagen

Ernst, R.E., Baragar, W.R.A. (1992) Evidence from magnetic fabric for the flow pattern of magma in the Mackenzie giant radiating dyke swarm. *Nature*, *356*, 511-513.

Ernst, R.E., Head, W.J., Parfitt, E., Grosfils, E. and Wilson, L., (1995), Giant radiating dike swarms on Earth and Venus, *Earth Sci. Rev.*, *39*, 1-58,.

Favela, J. and D.L. Anderson (1999), Extensional tectonics and global volcanism, *Editrice Compositori*, edited by E. Boschi, G. Ekstrom, and A. Morelli, pp. 463-498, Bologna, Italy,

Fleitout, L., Froidevaux, C., Yuen, D., (1986), Active lithosphere thinning: *Tectonophysics, 132*, 271-278.

Fiske, R.F, Jackson, E.D., (1972), Orientation and growth of Hawaiian volcanic rifts: the effect of regional structure and gravitational stresses, *Proc. Roy. Soc. Lond., 329*, 299-326.

Foulger, G.R., (2002), Plumes, or plate tectonic processes?, *Astron. Geophys*., *43*, 6.19-6.23,.

Foulger, G.R. and D.L. Anderson (2005) A cool model for the Iceland hotspot, *J. Volc. Geotherm. Res., 141*, 1-22,.

Fyfe, W.S., (1990), Magma underplating of continental crust: *Journal of Volcanology and Geothermal Research, 50*, 33-40.

Gac, S., Geoffroy, L., (2005), Axial magnetic anomaly segmentation along the East-Greenland volcanic passive margin compared to the magnetic segmentation of the Mid-Atlantic Ridge: a similar origin? *Geophysical Research Abstract, 7*, 7049.

Geoffroy, L., Bergerat, F., Angelier, J., (1993), Modification d'un champ de contrainte régional par un champ de contraintes magmatiques local. Exemple de l'Ile de Skye (Ecosse) au Paléocène: *Bulletin de la Société Géologique de France, 164*, 541-552.

Geoffroy L., Bergerat, F., Angelier, J., (1994), Tectonic evolution of the Greenland-Scotland ridge during the Paleogene, *New constraints: Geology, 22*, 653-656.

Geoffroy, L., Aubourg, C., (1997), Mantle cylinders as rift-zone initiators in continental crust: the British Tertiary Volcanic Province as a case study, EUG IX, Strasbourg.

Geoffroy, L., Olivier, Ph. Rochette, P., (1997), Structure of a hypovolcanic acid complex inferred from magnetic susceptibility anisotropy measurement: the Western Red Hills granites (Skye, Scotland, Thulean Igneous Province), *Bulletin of Volcanology, 59*, 147-159.

Geoffroy, L. (1998), Diapirism and intraplate extension: cause or consequence? *Académie des Sciences, Comptes Rendus, 326*, 267-273.

Geoffroy, L., Callot, J.P., Aubourg, C., Moreira, M., (2002), Magnetic and plagioclase linear fabric discrepancy in dykes : a new way to define the flow vector using magnetic foliation, *Terra Nova, 14*, 183-190.

Geoffroy, L., (2005), Volcanic passive margins: *Comptes Rendus Géosciences, 337*, 1395-1408.

Gernigon, L., Ringenbach, J.C., Planke, S., Le Gall, B., (2004), Deep structures and breakup along volcanic rifted margins: Insights from integrated studies along the outer Vøring Basin (Norway), *Marine and Petroleum Geology, 21*, 363-372.

Green, D. H., T. J. Falloon, S.M. Eggins and G.M. Yaxley. (1999). Primary magmas and mantle temperatures. *European J. Min. 13*, 437-451

Hargraves, R.B., Johnson, D. and Chan, C.Y., (1991), Distribution anisotropy: the cause of AMS in igneous rocks? *Geophysical Research Letters, 18*, 2193-2196.

Herrero-Bervera, E., Walker, G.P.L., Canon-Tapia, E., Garcia, M.O., (2001), Magnetic fabric and inferred flow direction in dikes, conesheets and sill swarms, Isle of Skye, *Scotland: Journal of Volcanology and Geothermal Research, 106*, 195-210.

Hill, R.I., Campbell, I.H., Davies, G.F., Griffiths, R.W., (1992), Mantle Plumes and Continental Tectonics*, Science, 256*, 186-193.

Hitchen, K. and Richtie, J.D., (1993), New K-Ar ages and a provisional chronology for the offshore part of the British Tertiary Igneous Province, *Scottish Journal of Geology, 29*, 73-85.

Hofton, M.A. and G.R. Foulger, (1996), Post-rifting anelastic deformation around the spreading plate boundary, north Iceland, 2: Implications of the model derived from the 1987-1992 deformation field, *Journal of Geophysical Research*, **101**, 25,423-25,436.

Holbrook, W. S., Larsen, H. C., Korenaga, J., Dahl-Jensen, T., Reid, I. D., Kelemen, P. B., Hopper, J. R., Kent, G. M., Lizarralde, D., Bernstein, S., Detrick, R. S., (2001), Mantle thermal structure and active upwelling during continental breakup in the North Atlantic, *Earth and Planetary Science Letters, 190*, 251-266.

Irvine, T.N., Andersen, J.C., Brooks, C.K., (1998), Included blocks (and blocks within blocks) in the Skaergaard intrusion: Geologic relations and the origins of

rhythmic modally graded layers, *GSA Bulletin, 110*, 1398-1447.

Jaupart, C., Mareschal, J.C., (1999), The thermal structure and thickness of continental roots, *lithos, 48*, 93-114.

Jones, E.J.W., Ramsay, A.T.S., Preston, N.J., Smith, A.C.S., (1974), A Cretaceous guyot in the Rockall Trough, *Nature, 251*, 129-131.

Jónsson, S., H. Zebker, P. Cervelli, P. Segall, H. Garbeil, P. Mouginis-Mark, Rowland, S., (1999), A shallow-dipping dike fed the 1995 flank eruption at Fernandina volcano, Galápagos, observed by satellite radar interferometry: *Geophysical Res. Lett.*, *26(8),* 1077–1080.

Juteau, T., Maury, R., (1999), *The oceanic crust : from accretion to mantle recycling*, edited by Springer-Verlag, 390p ,

Karson, J. A., Brooks, C. K., (1999), Structural and magmatic segmentation of the Tertiary east Greenland volcanic rifted margin, *J.F. Dewey Volume On Continental Tectonics.,* edited by P. Ryan, C. McNiocaill , *164*, pp. 313-318 , Geol. Soc. Sp. Publ.

Keen, C.E., Boutilier, R.R., (1995), Lithosphere-Asthenosphere interactions below rifts, *Rifted Ocean-Continent Boundaries*, edited by Banda E.,, pp. 17-30, Kluwer Academic Publishers.

Keen, C.E. and Boutilier, R.R., (1999), Small-scale convection and divergent plate boundaries, *Journal of Geophysical Research, 104*, 7389-7403.

Kelemen, P.B., Holbrook, W.S., (1995), Origin of thick, high-velocity igneous crust along the U.S. East Coast Margin, *Journal of Geophysical Research, 100*, 10077-10094.

Kent, R.W., Storey, M., Saunders, A.D., (1992), Large igneous provinces: sites of plume impact or plume incubation?, *Geology, 20*, 891-894.

Kent R.W., Fitton J.G., (2000), Mantle sources and melting dynamics in the British Palaeogene Igneous Province, *Journal of Petrology, 41*, 1023-1040.

Kerr, A.C., (1994), Lithospheric thinning during the evolution of continental large igneous provinces: A case study from the North Atlantic Tertiary Province, *Geology, 22*, 1027-1030.

King, S.D., Anderson, D.L., (1998), Edge-driven convection, *EPSL, 160*, 289-296.

Kirton, S.R, Donato, J.A., ()1985), Some buried Tertiary dykes of Britain and surrounding waters deduced by magnetic modelling and seismic reflection methods: *Journal of the Geological Society*, *142*, 1047-1057, London

Knight, M.D., Walker, G.P.L.,, (1988). Magma flow directions in dikes of the Koolau complex, Oahu, determined from magnetic fabric studies: *J. Geophys. Res., 93*,

4301-4319.

Korenaga, J., Holbrook, W.S., Kent, D.-V., Kelemen, P.B., Detrick, R.S., Larsen, H.C., Hopper, J. R., Dahl-Jensen, T., (2000), Crustal structure of the southeast Greenland margin from joint refraction and reflection seismic tomography: *Journal of Geophysical Research, 105*, 21591-21614.

Larsen, H.C. (1978), Offshore continuation of the East Greenland dyke swarm and North Atlantic Ocean formation, *Nature, 274*, 220-223.

Larsen, T.B., Yuen, D.A., Storey, M., (1999), Ultrafast mantle plumes and implications for flood basalt volcanism in the Northern Atlantic Region, *Tectonophysics, 311*, 31-43.

Lenoir, X., Feraud, G., Geoffroy, L., (2003), High-rate flexure of the East Greenland volcanic margin : constraints from $^{40}Ar/^{39}Ar$ dating of basaltic dykes, *Earth and Planetary Science Letters*, 1-14.

Lin, J., Purdy, G.M., Schouten, H., Sempere, J.C., Zervas, C., (1990), Evidence from gravity data for focused magmatic accretion along the Mid-Atlantique Ridge, *Nature*, *334*, 627-632.

Lustrino, M., (2005), How the delamination and detachment of lower crust can influence basaltic magmatism, *Earth-Science Reviews, 72, 21-38.*

Macdonald, R., Wilson, L., Thorpe, R.S., Martin, A., (1988), Emplacement of the Cleveland Dyke: Evidence from geochemistry, Mineralogy, and Physical Modelling: *Journal of Petrology, 29*, 559-583.

Madge, L. S., Sparks, D.W., R.S. Detrick, (1997), The relationship between buoyant mantle flow, melt migration, and gravity bull's eyes at the Mid-Atlantic Ridge between 33°N and 35°N, *Earth and Planetary Science Letters, 148*, 59-67.

Mattey, D.P., Gibson, J.L., Marriner, G.F., Thompson, R.N., (1977), The diagnostic geochemistry, relative abundance and spatial distribution of high-calcium, low alkali olivine tholeiitic dykes in the Lower Tertiary regional swarm of the Isle of Skye, NW Scotland, *Mineralogical Magazine, 41*, 273-285.

J. Gregory McHone, Don L. Anderson and Yuri A. Fialko, (2004) Giant dikes: patterns and plate tectonics in Do Plumes exist? www.mantleplumes.org/

McLeod, P., Tait, Stephen, (1999), The growth of dykes from magma chambers, *Journal of Volcanology and Geothermal Research, 92*, 231-245.

Moreira, M., Geoffroy, L., Pozzi, J.P., (1999), Ecoulement magmatique dans les dykes du point chaud des Açores: étude par anisotropie de susceptibilité magnétique, *Comptes Rendus de l'Académie des Sciences de Paris, 329*, 15-22.

Morency, C., Doin, C., Dumoulin, C., (2002), Convective destabilization of a

thickened continental lithosphere, *Earth and Planetary Science Letters, 202*, 303-320.

Morgan, W.J., (1972), Convection plumes in the lower mantle, *Nature, 230*, 42-43.

Morgan, JP., (1987), Melt migration benath mid-ocean spreading centers: *Geophysical Research Letters, 14*, 1238-1241.

Mutter, J.C., Buck, W.R., Zehnder, C.M., (1988), Convective partial melting, 1. A model for the formation of thick basaltic sequences during the initiation of spreading: *Journal of Geophysical Research, 93*, 1031-1048.

Myers, J.S., (1980), Structure of the coastal dyke swarm and associated plutonic intrusions of East Greenland, *Earth and Planetary Science Letters, 46*, 407-418.

Nicolas, A., (1990), Melt extraction from mantle peridotites: hydrofracturing and porous flow, with consequences for oceanic ridge activity, *Magma Transport and Storage ,* edited by Rhyan, pp.159-173, M.P., John Wiley and Sons Ltd.

Nicolas, A., (1992), Kinematics in magmatic rocks with special reference to gabbros: *Journal of Petrology, 33*, 891-915.

Nishimura, T., S Ozawa, M. Murakami, T. Sagiya,T.Tada, M. Kaidzu, M.Ukawa, (2001), Crustal deformation caused by magma migration in the northern Izu Islands, Japan, *Geophysical Research Letters, 28,* 3745-3748.

Olson, P., Nam, I.S., (1986), Formation of seafloor swells by mantle plumes, *Journal of Geophysical Research, 91*, 7181-7192.

Parfitt, E.A., Gregg, T.K.P., Smith, D.K., (2002), A comparison between subaerial and submarine eruptions at Kilauea Volcano, Hawaii: implications for the thermal viability of lateral feeder dikes, *Journal of Volcanology and Geothermal Research, 113*, 213-242.

Pavlenkova, G.A., Priestley, K., Cipar, J., (2002), 2D model of the crust and uppermost mantle along rift profile, Siberian Craton, *Tectonophysics, 355,* 171-186.

Philpotts, A.R., Asher, P.M., (1994), Magmatic flow-direction indicators in a giant diabase feeder dike, *Geology*, *22*, 363-366.

Planke, S., Symonds, P.A., Alvestad, E., Skogseid, J., (2000), Seismic volcanostratigraphy of large-volume basaltic extrusive complexes on rifted margins: *J. Geophys. Res.,105*, 19335-19352.

Rhyan, M.P., (1987), Neutral buoyancy and the mechanical evolution of magmatic systems, *Magmatic processes : physicochemical principles*, edited by Mysen, B.O., *1*, pp. 259-287, Geochemistry Society Special Publication.

Richards, M.A., Duncan, R.A., Courtillot, V., (1989), Flood basalts and hot-spot tracks: plume heads and tails, *Science, 246,* 103-107.

Roberts, DG, (1974), Structural development of the British Isles, the continental. margin, and the Rockall Plateau, *The geology of continental margins* , edited by Burk, C.A., Drake, C.L., Springer Verlag, pp. 343-359, New-York.

Roberts, D.G., Morton, A.C., Murray, J.W., Keene, J.B., (1979), Evolution of volcanic rifted margins: synthesis of Leg 81 results on the West margin of Rockall plateau, *Initial Reports, DSDP,81*, 883-911.

Rochette, P., Jenatton, L., Dupuy, C., Boudier, F., Reuber, I., (1991), Diabase Dikes Emplacement in the Oman Ophiolite: a Magnetic Fabric Study with Reference to Geochemistry, *Ophiolite Genesis and Evolution of the Oceanic Lithosphere*, edited by Peters, T.J. et al., pp. 55-82.

Rohrman, M., Van der Beck, P., (1996), Cenozoic postrift domal uplift of North-Atlantic margins: an asthenospheric diapirism model, *Geology, 24*, 901-904.

Rubin, A.M., (1993), Dikes vs. diapirs in visco-elastic rock, *Earth and Planetary Science Letters, 119*, 641-659.

Saunders, A. D., Fitton, J. G., Kerr, A. C., Norry, M. J., Kent, R. W., (1997), The North Atlantic igneous province, In Large Igneous Provinces, *Continental, Oceanic, and Planetary Flood Volcanism*, edited by J. J. Mahoney, M. F. Coffin, *100*, pp. 45-93, AGU Geophysical Monograph, Washington.

Scheck-Wenderoth, M., Faleide, J.I., Raum, T., Mjelde, R., Di Primo, R. and Horsfield, B., (2006), Results from 2D/3D structural modeling of the Norwegian margin, ILP Task Force on sedimentary basin, Québec 18-22th September, p. 58.

Schmeling, H., (2000), Partial melting and melt segregation in a convecting mantle, *Physics and Chemistry of Partially Molten Rocks*, edited by N. Bagdassarov, D. Laporte, A.B. ,pp. 141 – 178, Thompson Kluwer Academic Publ., Dordrecht,.

Self, S., Thordarson, T., Keszthelyi, L., (1997), Emplacement of continental flood basalt lava flows. Large Igneous Provinces, *Continental, Oceanic, and Planetary flood volcanism,* edited by J.-J. Mahoney et M.-F. Coffin, *100*, pp. 381-410, AGU Geophysical Monograph, Washington.

Shaw, H.R., (1980), The fracture mechanism of magma transport from the mantle to the surface, *Physics of Magmatic Processes* , edited by Hargraves, R.B., pp. 201-264, University Press, Princeton.

Shelley, D., (1985), Determining paleo-flow directions from groundmass fabrics in the Lyttelton radial dykes, *Journal of Volcanological and Geothermal Research, 25*, 69-79, New Zealand.

Sheth, H.C., (1999), A historical approach to continental flood basalt volcanism:

insights into pre-volcanic rifting, sedimentation, and early alkaline magmatism, *Earth and Planetary Science Letters, 168,* 19-26.

Sigurdsson, H., (1987), Dike injection in Iceland: a review: *Geological Association of Canada., Special Paper, 34*, 55-64.

Smith, W. H. F., and D. T. Sandwell, Global seafloor topography from satellite altimetry and ship depth soundings, *Science, 277*, 1957-1962

Smythe, D.K., Chalmers, J.A., Skuce, A.G., Dobinson, A., Mould, A.S., (1983), Early opening history of the North Atlantic- I. Structure and origin of the Faeroe-Shetland Escarpment, *Geophysical Journal of the Royal Astronomy Society, 72*, 373-398.

Speight, J.M., Skelhorn, R.R., Sloan, T. and Knapp, R.J. (1982), *The dike swarms of Scotland*, editted by John Wiley and Son, pp. 449-459, Sutherland.

Spera, F.J., (1980), Aspects of magma transport, *Physics of Magmatic Processes*, edited by Hargraves, R.B., pp. 265-318, Princeton University Press, Princeton.

Speigelman, M. and Reynolds, J.R., (1999), Combined dynamic and geochemical evidences for convergent melt flow beneath the east Pacific Rise, *Nature, 402*, 282-285.

Staudigel, H., Gee, J. Tauxe, L., Varga, R.J. (1992), Shallow intrusive directions of sheeted dikes in the Troodos ophiolite: Anisotropy of magnetic susceptibility and structural data, *Geology, 20*, 841-844.

Thompson, R.N., Morrison, M.A., (1988), Asthenospheric and lower lithospheric mantle contributions to continental extensional magmatism: an example from the British Tertiary Province, *Chem. Geol., 68*, 1-15.

Thompson, R.N., Gibson, S.A., (1991), Subcontinental mantle plumes, hotspots and preexisting thinspots, *Journal of the Geological Society, 148*, 973-977.

Tilling, R.I. and Dvorak, J.J., (1993), Anatomy of a basaltic volcano, *Nature: 363*, 125-133.

Vann, I.R., (1978), The sitting of Tertiary volcanicity, *Crustal evolution in northwestern Britain and adjacent regions*, edited by Bowes, D.R., Leake, B.E, *10*, 393-414, Journal of The geological society of London, Special Issue.

Van Wijk, J.W., R.S. Huismans, M. Ter Voorde and S.A.P.L. Cloetingh, (2001), Melt generation at volcanic continental margins: no need for a mantle plume? *Geophysical Research Letters*, 28, 3995-3998.

Van Wijk, J.W., Cloetingh, S.A.P.L., (2002), Basin migration caused by slow lithospheric extension, *Earth and Planetary Science Letters*, 198, 275-288.

Varga, R. J., Gee, J.S., Staudigel, H., Tauxe, L., (1998), Dike surface lineations as magma flow indicators within the sheeted dike complex of the Troodos Ophiolite, Cyprus, *J. of Geophys. Res., 103*, 5241-5256.

Weinberg, R.F., Podlachikov, Y.Y., (1995), The rise of solid-state diapirs, *Journal of Structural Geology, 17*, 1183-1195.

White, N., Lovell, B., (1997), Measuring the pulse of a plume with the sedimentary record, *Nature, 387*, 888-891.

White, R.S., Spence, G.D., Fowler, S.R., McKenzie, D.P., Westbrook, G.K., Bowen, A.N., (1987), Magmatism at rifted continental margins, *Nature, 330*, 439-444.

White, R. S., McKenzie, D., (1989), Magmatism at rift zones: the generation of volcanic continental margins and flood basalts, *Journal of Geophysical Research, 94*, 7685-7729.

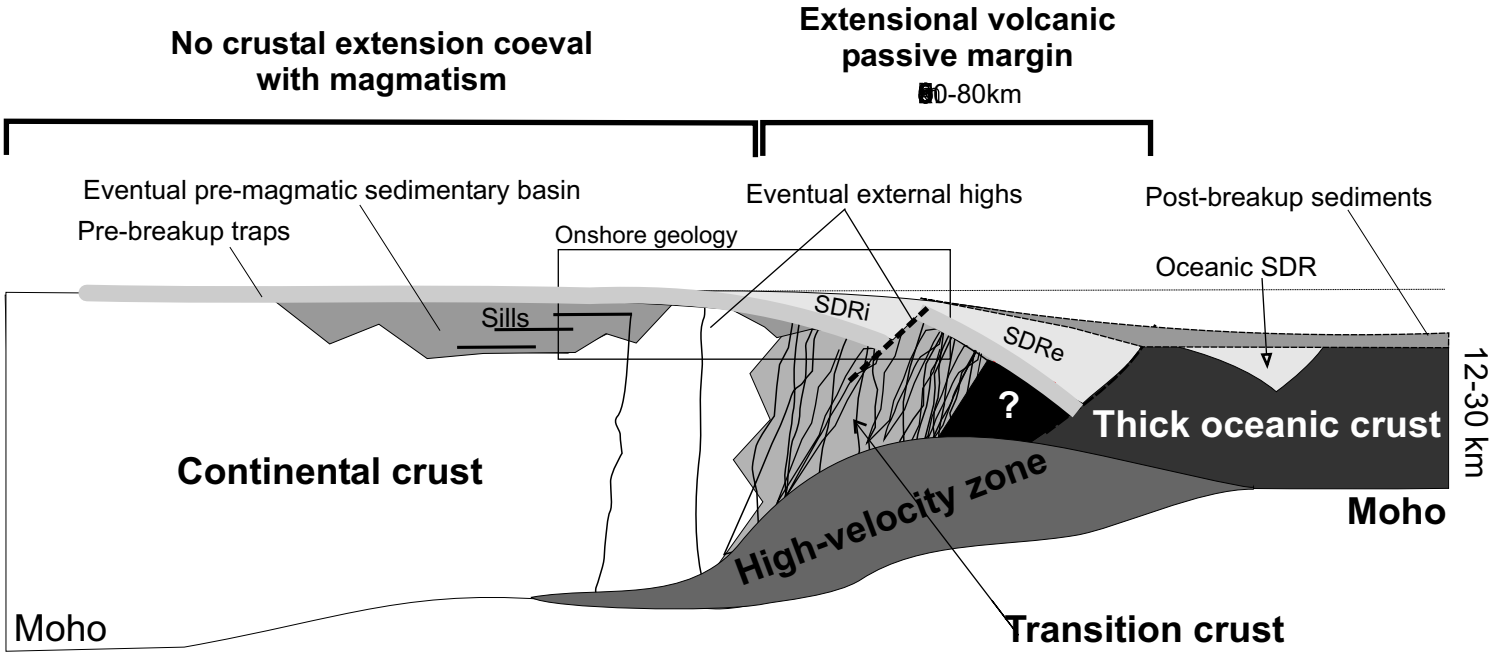

FIGURE 1

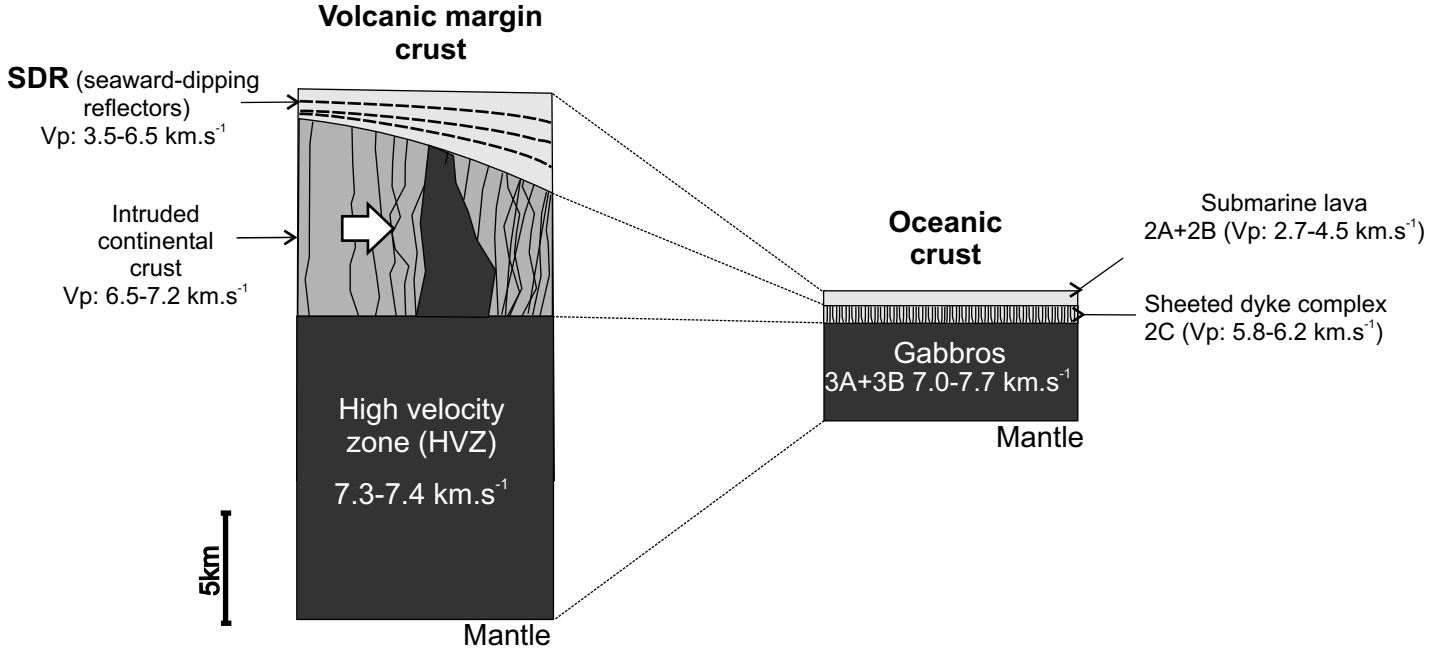

FIGURE 2

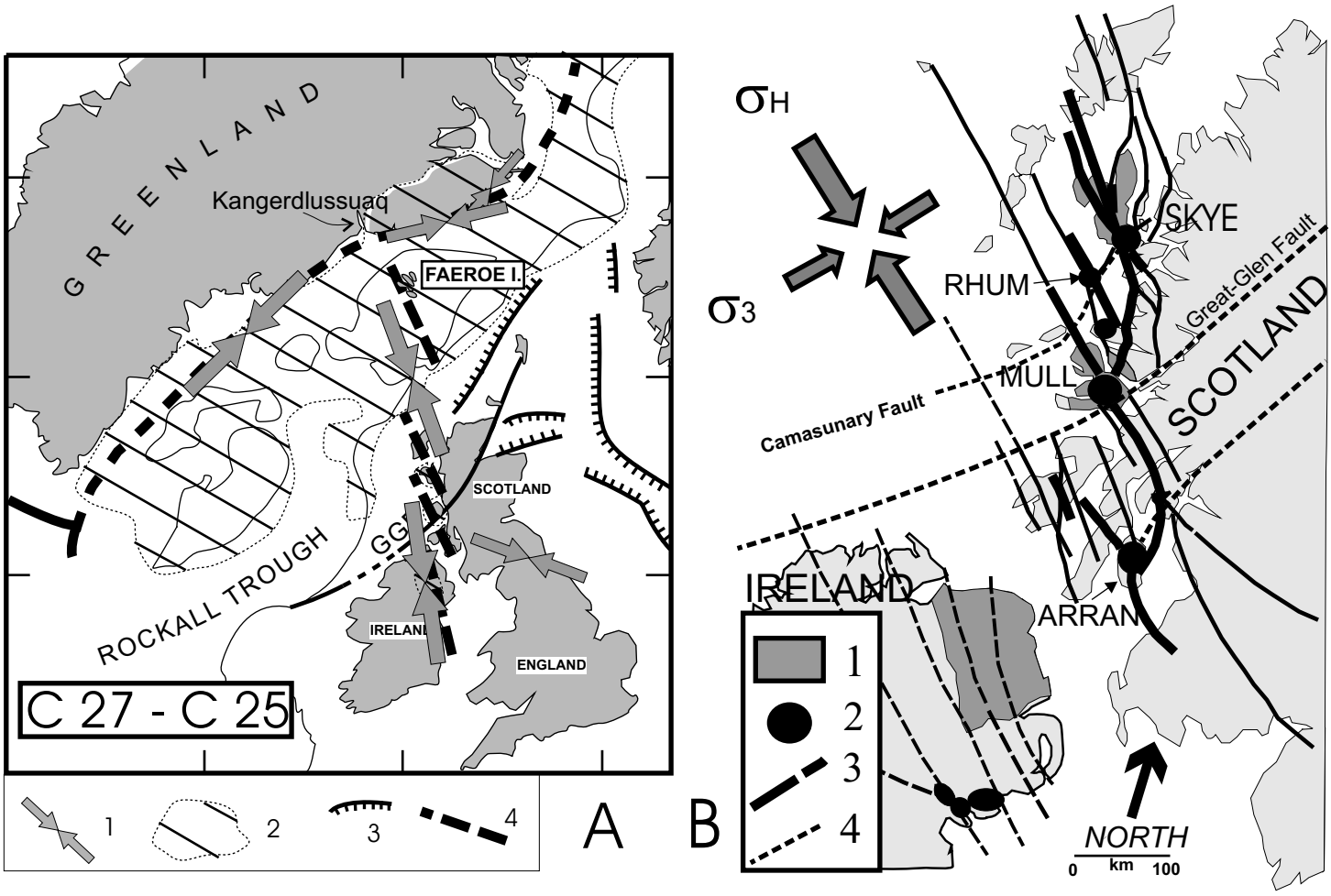
GREENLAND
Kangerdlussuaq
FAEROE I.
SCOTLAND
ROCKALL TROUGH
IRELAND
ENGLAND
C 27 - C 25
1
2
3
4
A
B
σH
σ3
RHUM
SKYE
Great-Glen Fault
MULL
Camasunary Fault
SCOTLAND
IRELAND
ARRAN
1
2
3
4
NORTH
0 km 100

FIGURE 3

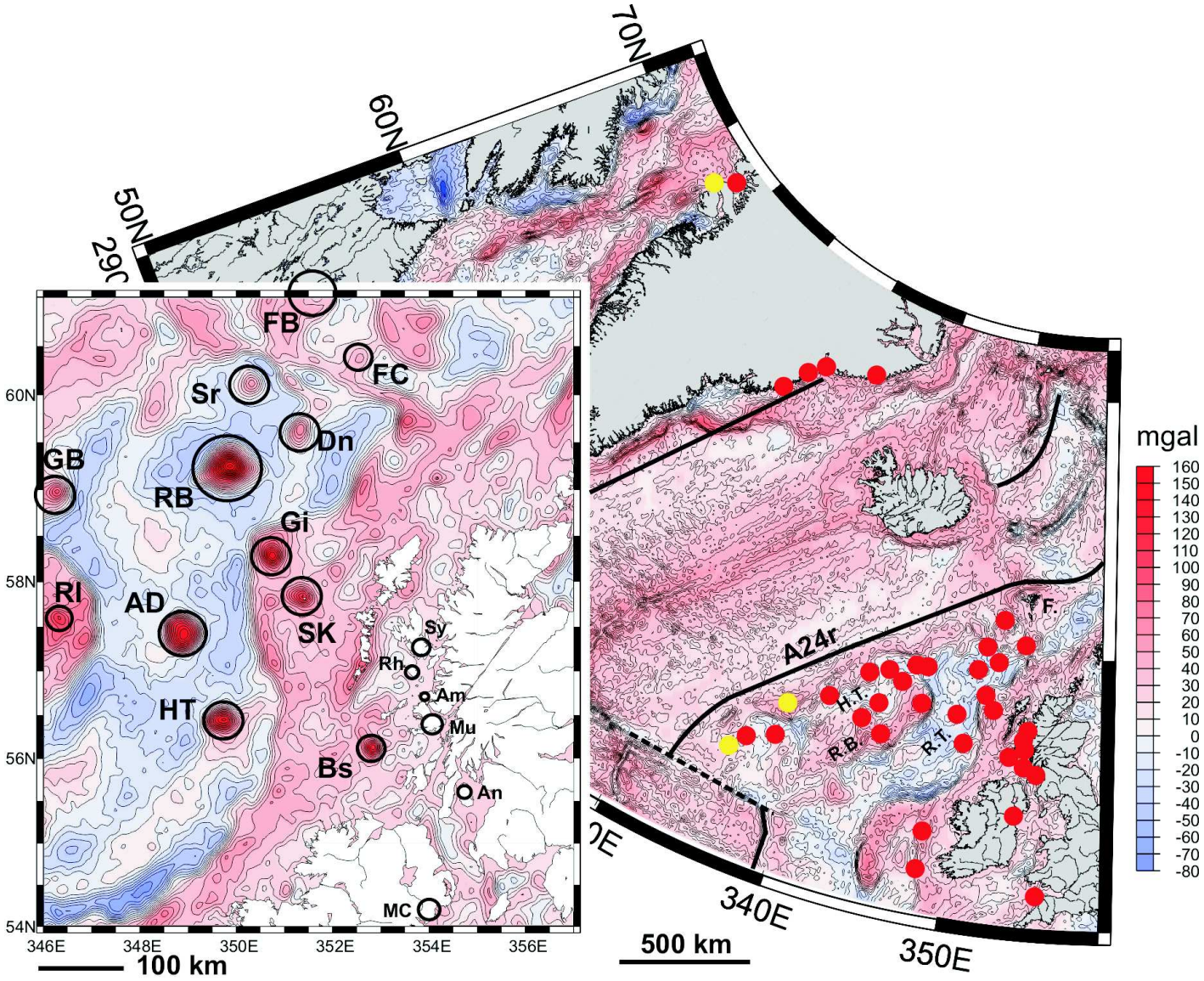
70N
60N
50N
29C
FB
FC
Sr
Dn
GB
RB
Gi
RI
AD
SK
Sy
Rh
Am
Mu
HT
Bs
An
MC
60N
58N
56N
54N
346E
348E
350E
352E
354E
356E
100 km
340E
350E
500 km
A24r
H.T.
R.B.
R.T.
F.
mgal
160
150
140
130
120
110
100
90
80
70
60
50
40
30
20
10
0
-10
-20
-30
-40
-50
-60
-70
-80

FIGURE 4

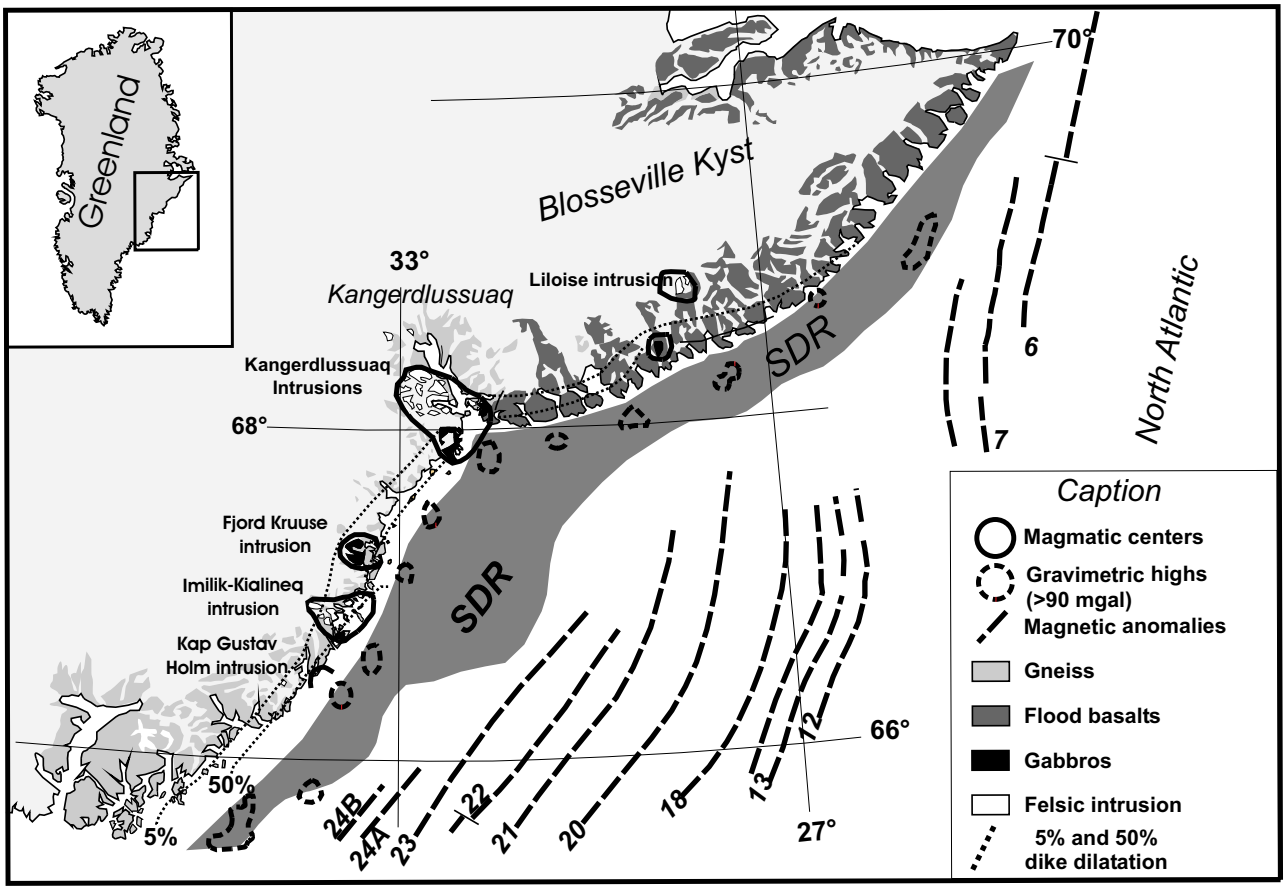
Greenland
Blosseville Kyst
70°
33°
Kangerdlussuaq
Liloise intrusion
Kangerdlussuaq
Intrusions
SDR
68°
North Atlantic
6
7
Fjord Kruuse
intrusion
Imilik-Kialineq
intrusion
Kap Gustav
Holm intrusion
SDR
66°
50%
5%
24B
24A
23
22
21
20
18
13
12
27°
Caption
Magmatic centers
Gravimetric highs
(>90 mgal)
Magnetic anomalies
Gneiss
Flood basalts
Gabbros
Felsic intrusion
5% and 50%
dike dilatation

FIGURE 5

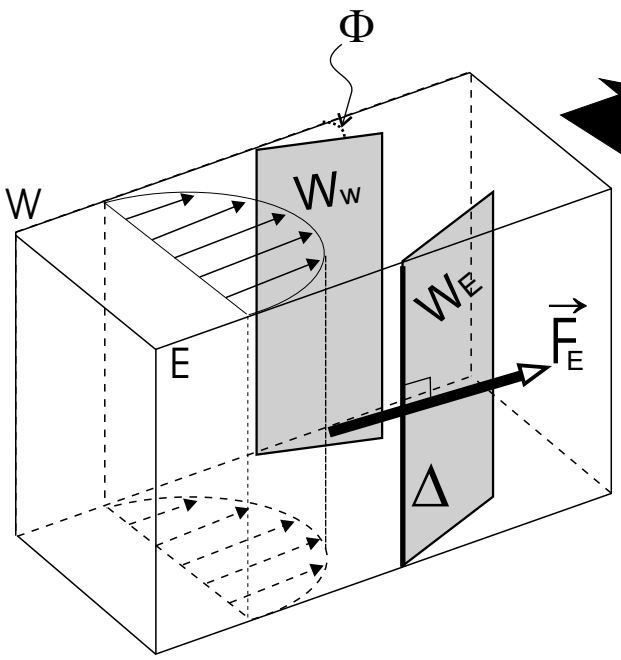

MAGMA FLOW DIRECTION (horizontal and towards the North in the figure)

A

W_E/W_w : magma foliation (grey plane), near E or W wall. Magma foliation is close to the AMS plane that contain the maximum and intermediate AMS axes K1 and K2 (i.e. Magnetic foliation)

Φ: imbrication angle between magma foliation and dike wall

Δ: intersection axis between magma foliation and dike wall

F_E: Flow vector, eastern wall of the dike

Horizontal flow (see A)

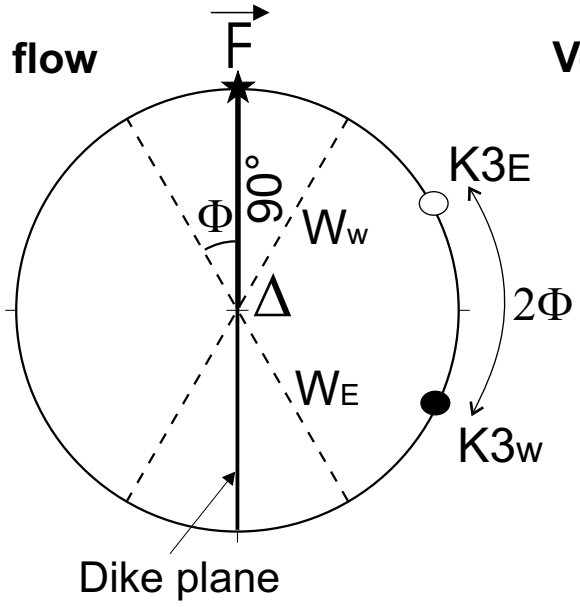

Vertical flow

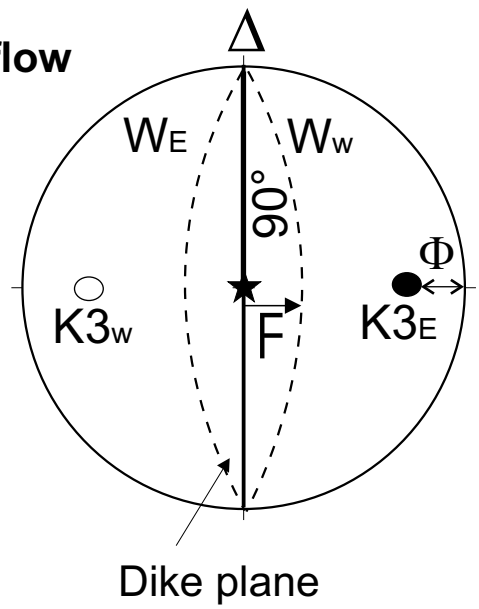

F: Flow vector (merged vectors from the eastern and western walls)
Note : with the above geometric method the orientation of the magnetic axes K1 and K2 is not taken into account any more)

B

Figure 6

FIGURE 7

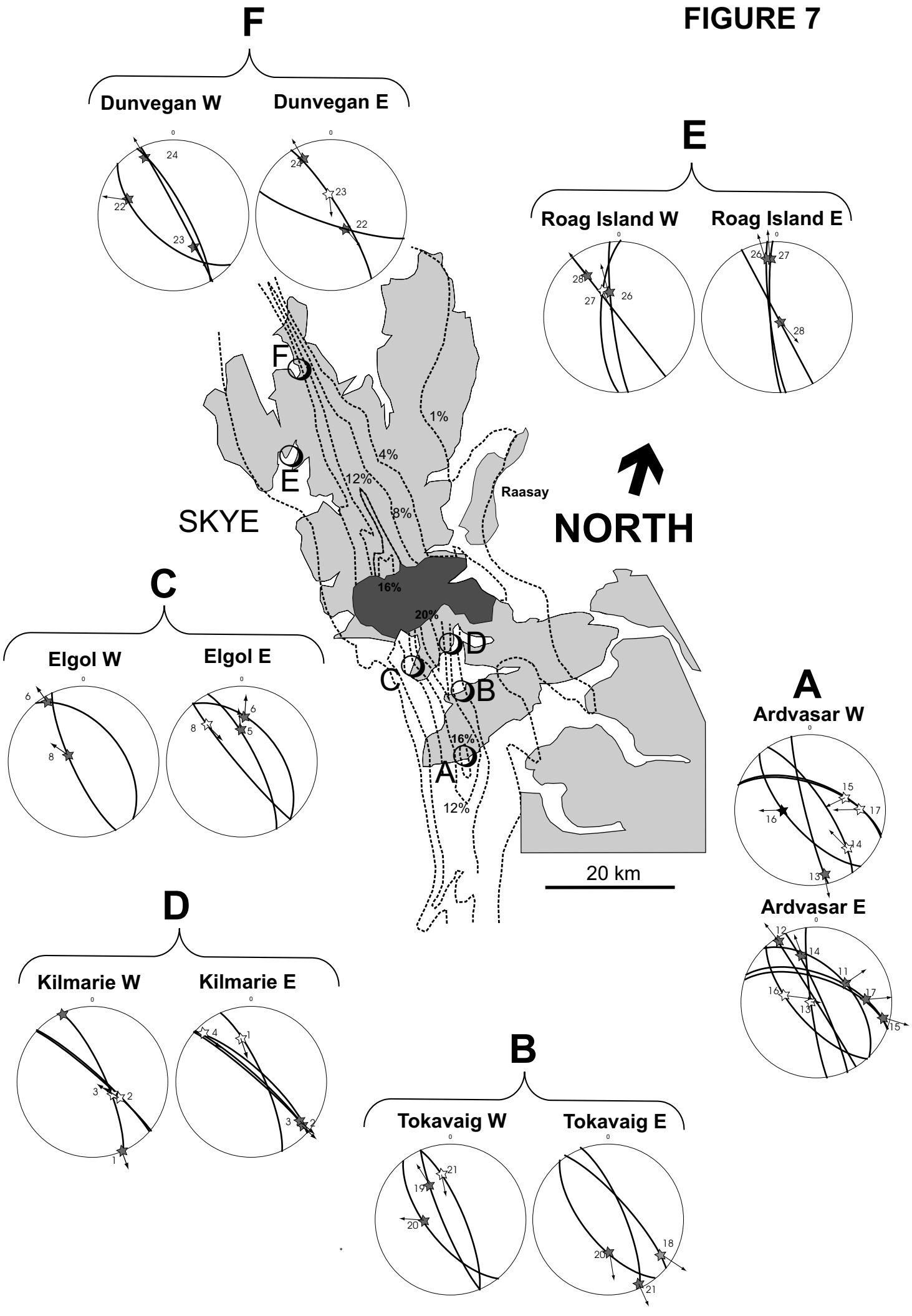
F
Dunvegan W
Dunvegan E
E
Roag Island W
Roag Island E
SKYE
Raasay
NORTH
1%
4%
8%
12%
16%
20%
C
Elgol W
Elgol E
A
Ardvasar W
Ardvasar E
D
Kilmarie W
Kilmarie E
B
Tokavaig W
Tokavaig E
20 km

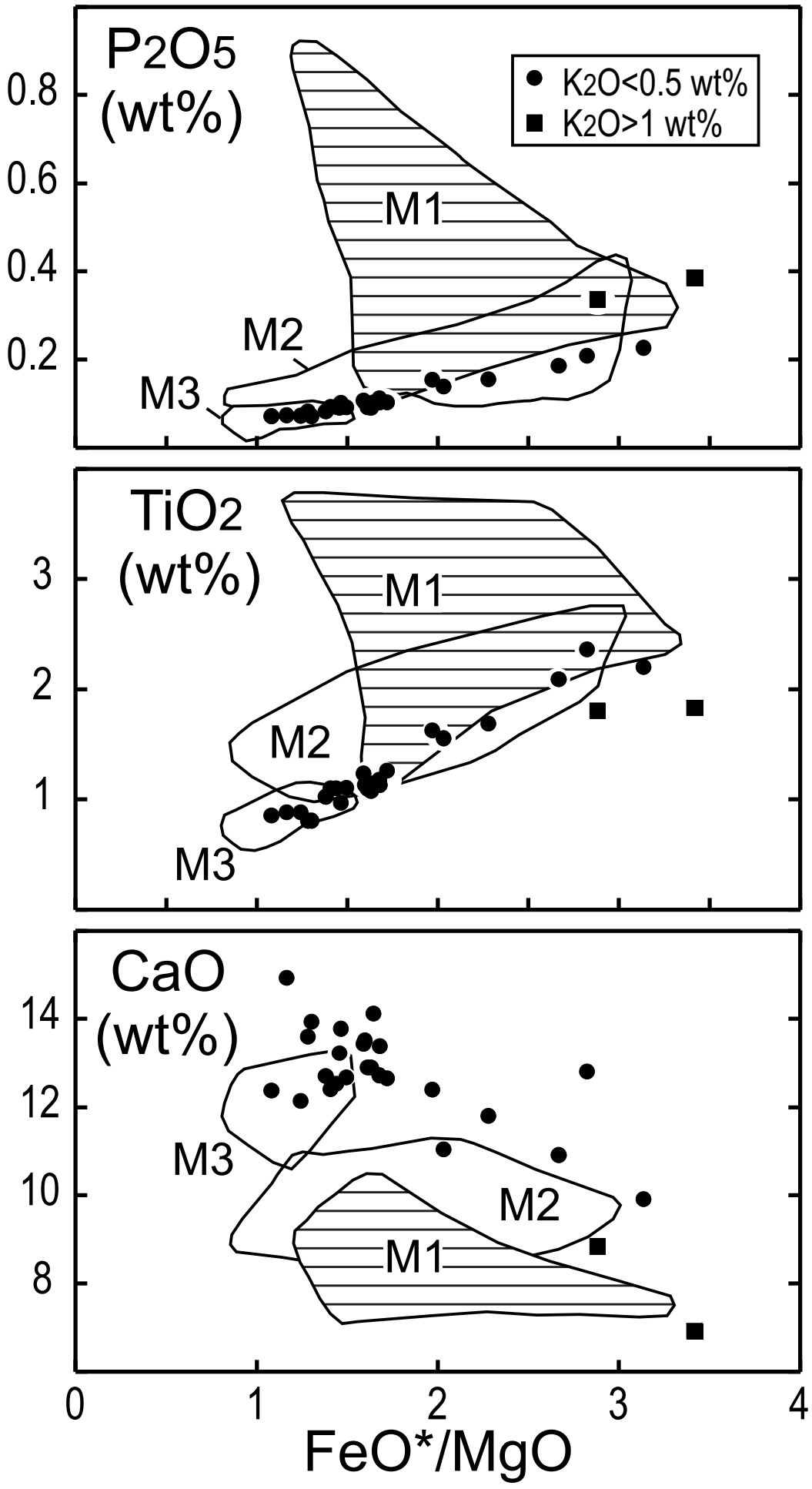
P2O5 (wt%)
K2O<0.5 wt%
K2O>1 wt%
M1
M2
M3
TiO2 (wt%)
M1
M2
M3
CaO (wt%)
M3
M2
M1
0.8
0.6
0.4
0.2
3
2
1
14
12
10
8
0
1
2
3
4
FeO*/MgO

Figure 8

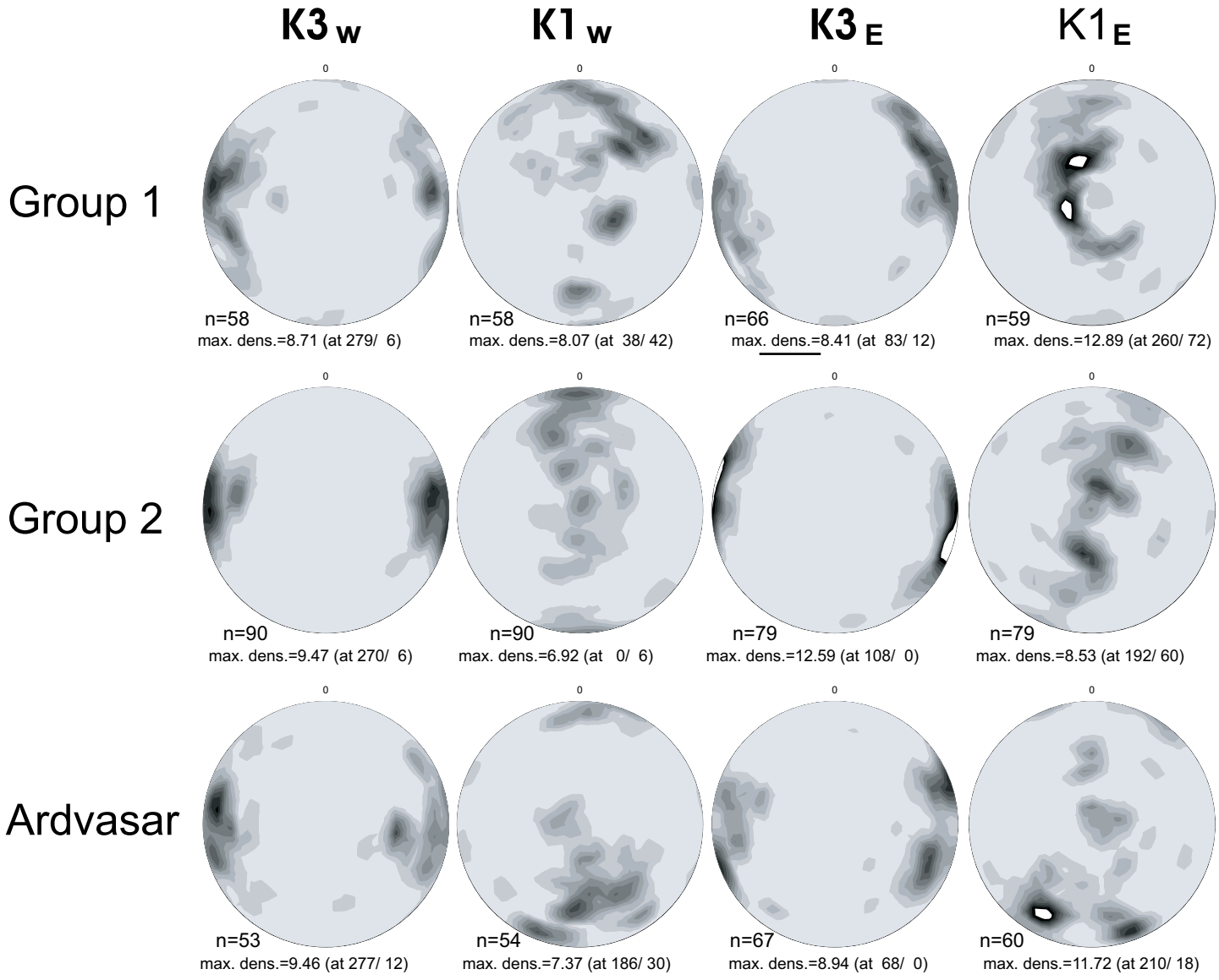

Figure 9 Geoffroy et al. GSA

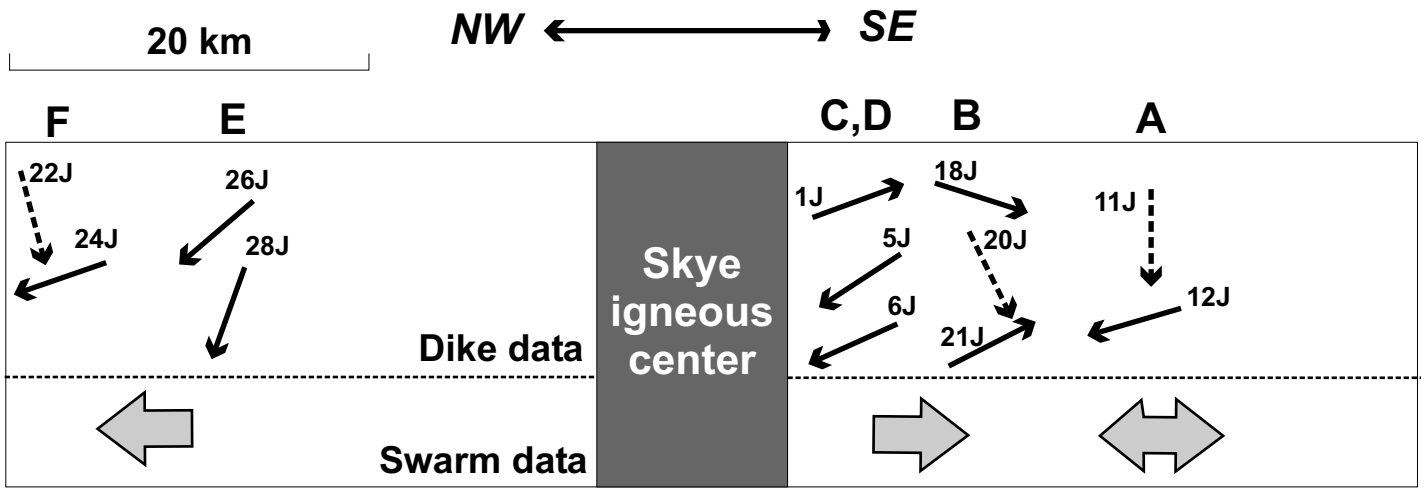

Data

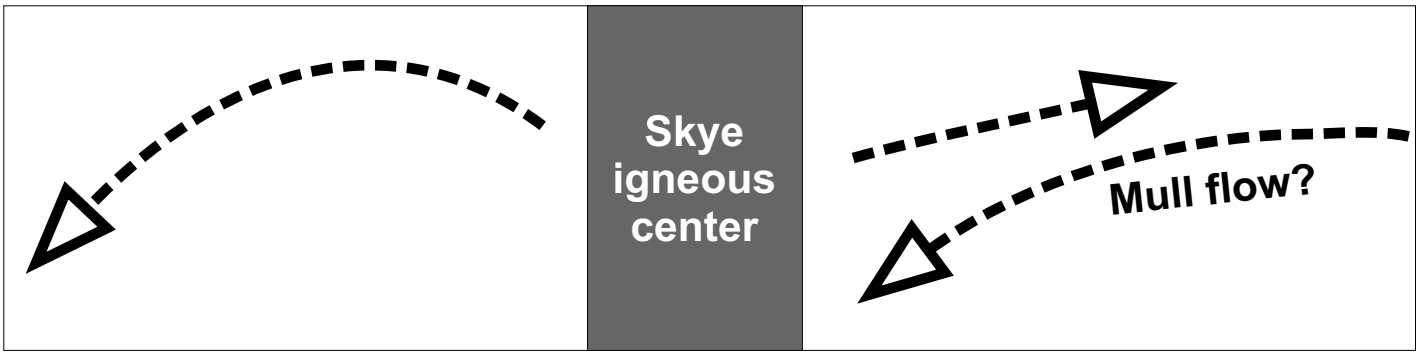

Interpretation

FIGURE 10

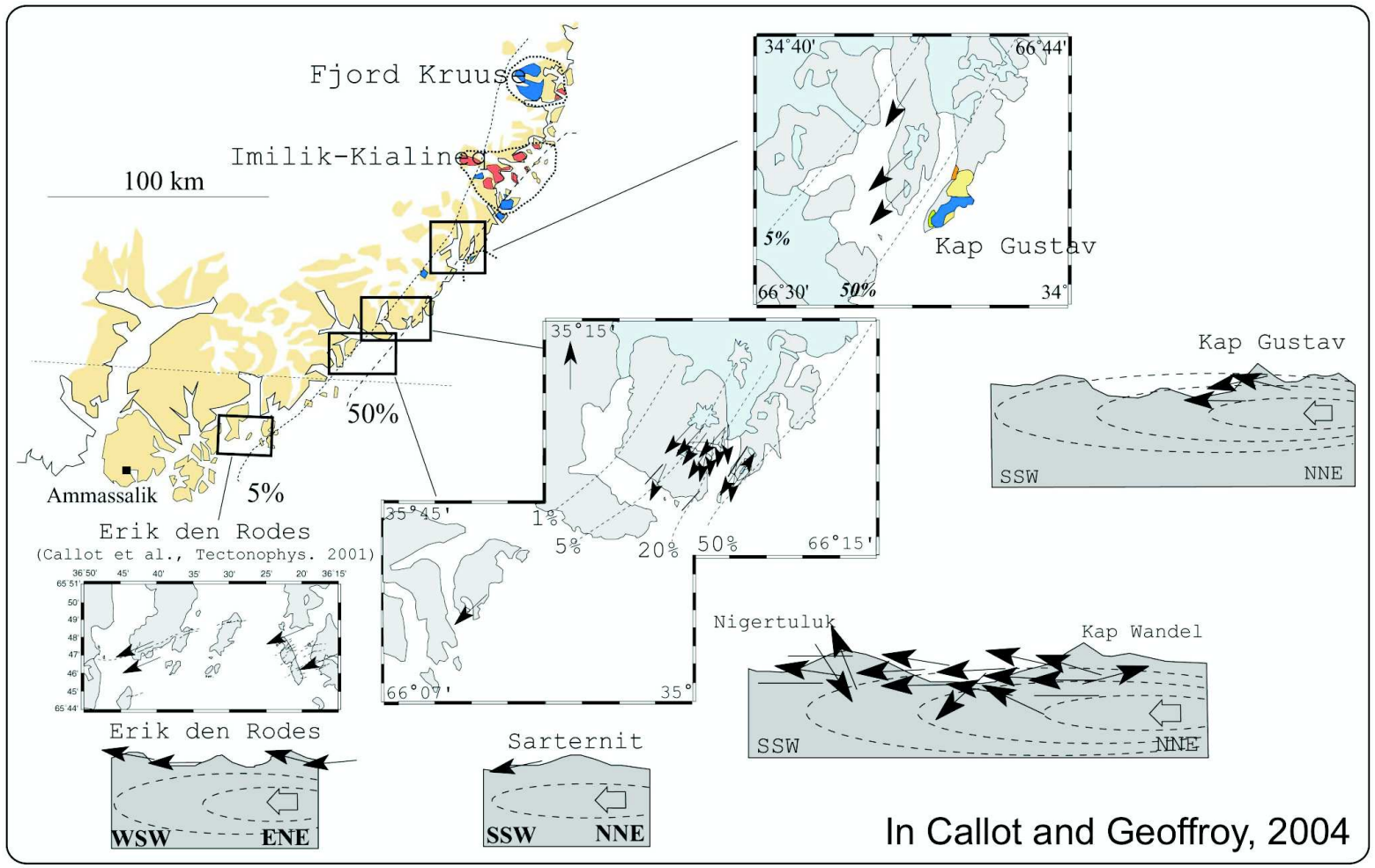
Fjord Kruuse
Imilik-Kialineq
100 km
Ammassalik
5%
50%
Erik den Rodes
(Callot et al., Tectonophys. 2001)
Erik den Rodes
WSW
ENE
34°40'
66°44'
5%
Kap Gustav
66°30'
50%
34°
35°15'
35°45'
1%
5%
20%
50%
66°15'
66°07'
35°
Kap Gustav
SSW
NNE
Nigertuluk
Kap Wandel
SSW
NNE
Sarternit
SSW
NNE
In Callot and Geoffroy, 2004

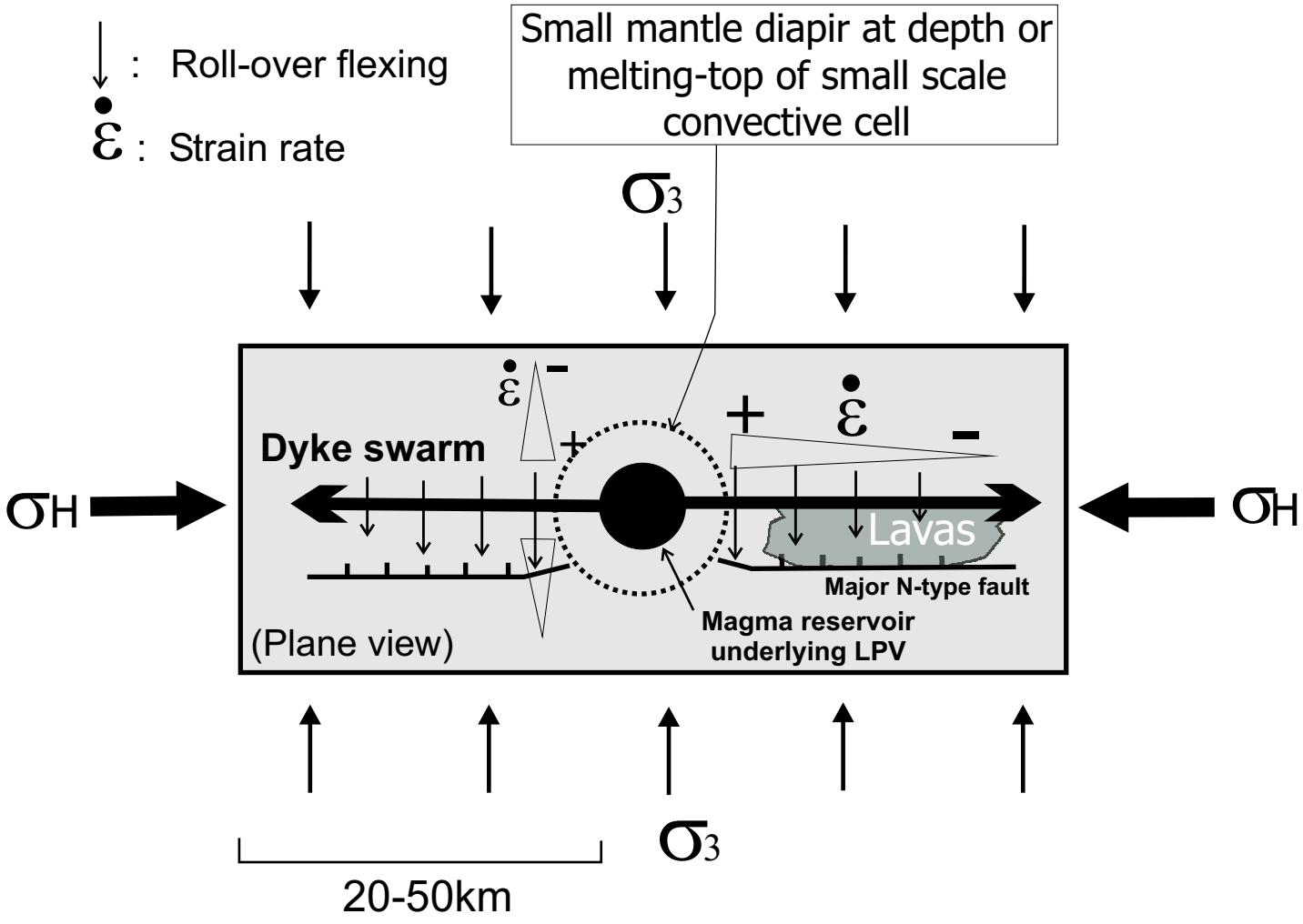
: Roll-over flexing
: Strain rate
Small mantle diapir at depth or melting-top of small scale convective cell
σ3
Dyke swarm
σH
σH
Lavas
Major N-type fault
Magma reservoir underlying LPV
(Plane view)
σ3
20-50km

FIGURE 12

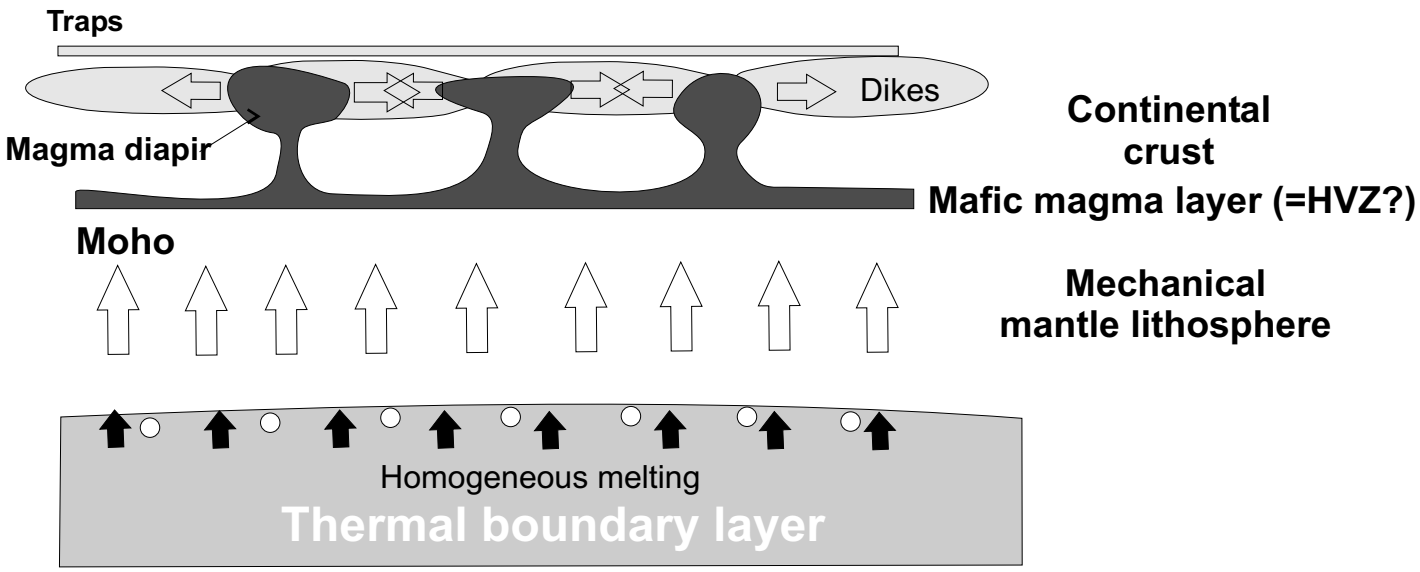

A .Traps origin: magma diapir hypothesis (rejected)

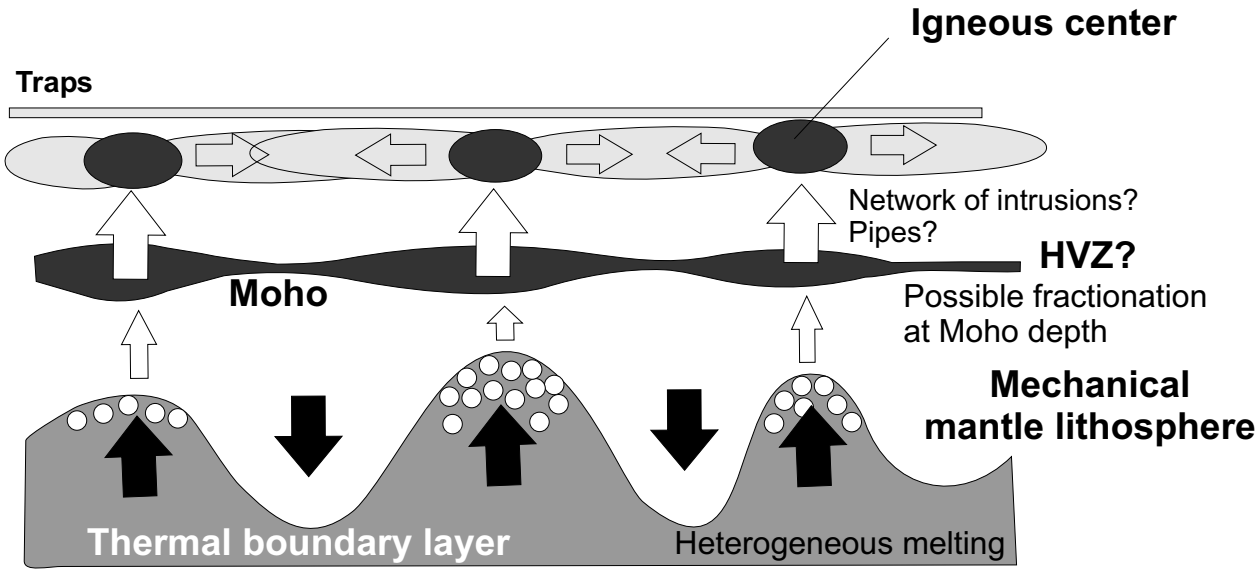

B. Traps origin: small-scale convection hypothesis (favored)

FIGURE 13

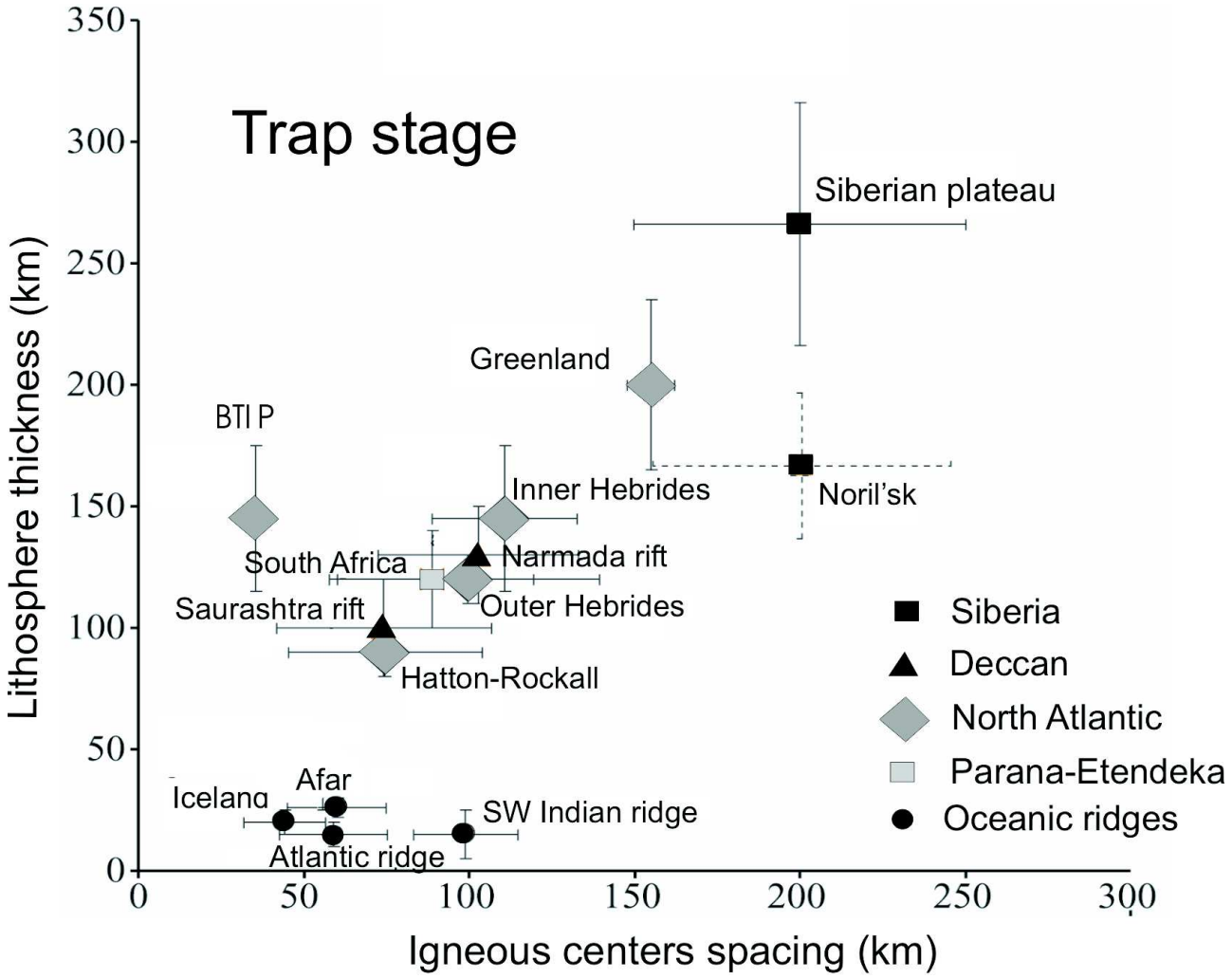
Trap stage
Siberian plateau
Greenland
BTI P
Inner Hebrides
Noril'sk
South Africa
Narmada rift
Saurashtra rift
Outer Hebrides
Hatton-Rockall
Afar
Iceland
SW Indian ridge
Atlantic ridge
Siberia
Deccan
North Atlantic
Parana-Etendeka
Oceanic ridges
Lithosphere thickness (km)
Igneous centers spacing (km)
0
50
100
150
200
250
300
350

Figure 14

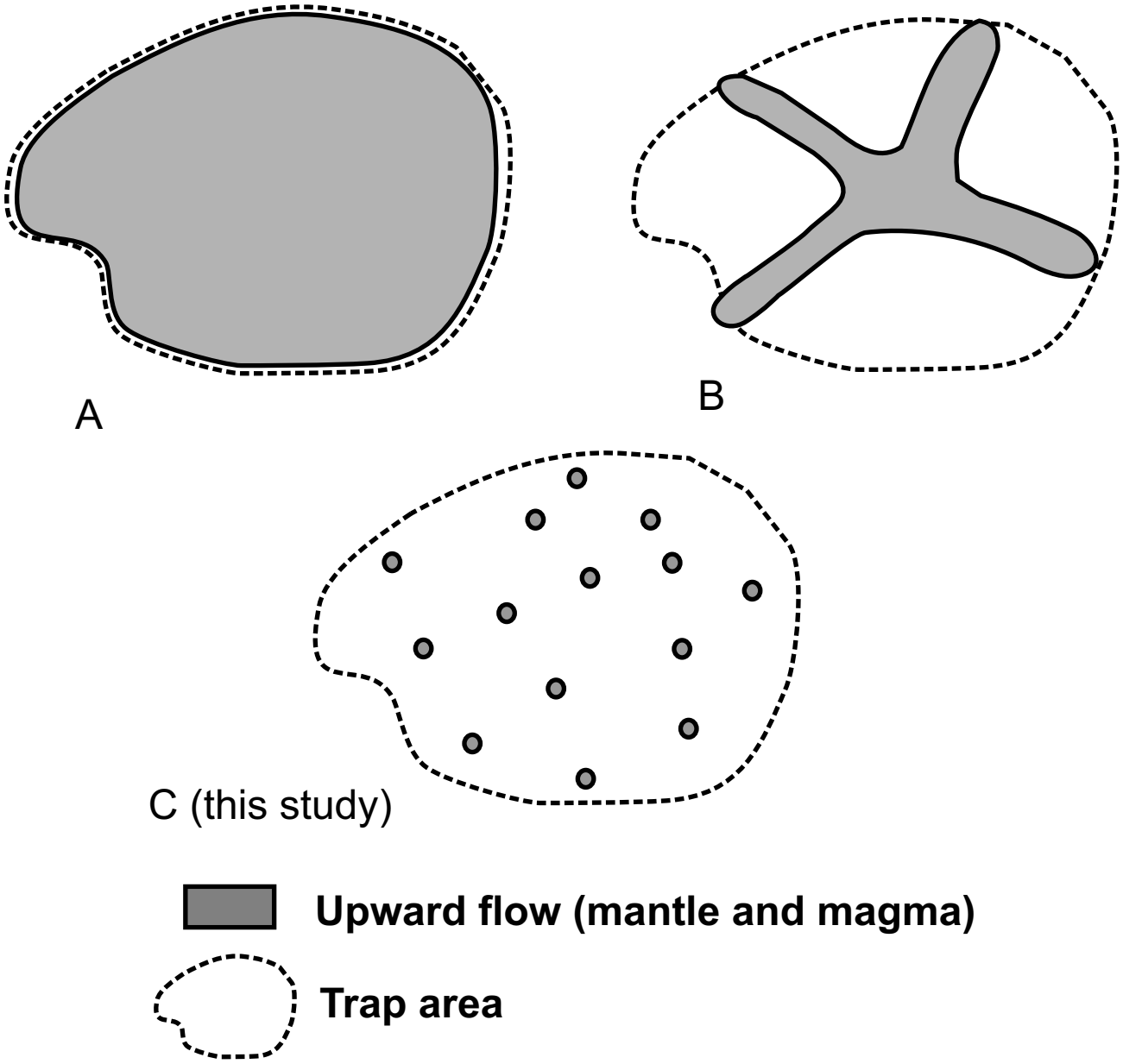

Figure 15

	SiO2	TiO2	Al2O3	Fe2O3	MnO	MgO	CaO	Na2O	K2O	P2O5	LOI	total	Sr
8J	46,25	1,63	13,2	15,45	0,25	6,1	11,4	2,12	0,08	0,15	3,09	99,72	135
9J	45,5	1,46	14,6	13,7	0,19	6,07	10,35	1,65	0,08	0,13	5,4	99,13	181
11J	44,5	2,27	14,15	14,5	0,19	4,62	12,3	3	0,28	0,2	3,77	99,78	211
4J	47,2	2,13	12,67	17	0,26	4,88	9,6	2,44	0,43	0,22	2,49	99,32	139
5J	48,1	1,72	13,92	14,12	0,23	4,41	8,42	2,84	1,11	0,32	4,39	99,58	341
7J	46,25	0,79	17,89	10,05	0,17	6,95	13,6	1,75	0,05	0,07	2,21	99,78	121
1J	46,4	1,23	13,84	13,94	0,23	7,3	12,35	1,99	0,15	0,1	1,91	99,44	116
2J	44,1	0,84	14,25	11,2	0,19	8,65	14,2	1,47	0,15	0,07	4,35	99,47	143
3J	44,25	1,16	14,75	11,9	0,25	6,74	12,6	1,9	0,12	0,1	5,82	99,59	147
18J	46,45	1,11	14,25	12,3	0,23	6,74	13,7	1,96	0,17	0,1	2,32	99,33	130
19J	47,5	1,05	14,25	12,7	0,21	7,85	13,05	1,88	0,04	0,09	1,3	99,92	105
20J	46,9	1,1	13,8	12,68	0,25	7,14	13,12	1,96	0,06	0,1	2,73	99,84	121
15J	47	0,95	15,8	11,4	0,19	7,01	13,5	1,95	0,11	0,1	1,94	99,95	141
16J	46,25	0,79	18,6	9,6	0,15	6,74	13,25	1,81	0,15	0,08	2,08	99,5	142
17J	51,35	1,76	14,05	13,1	0,19	3,45	6,65	3,1	1,94	0,37	3	98,96	420
12J	46,4	1,59	14,1	14,1	0,23	6,44	12,1	2,3	0,18	0,15	2,39	99,98	161
13J	47,9	1,16	14,13	13,1	0,22	7,03	12,5	1,94	0,19	0,11	1,59	99,87	131
14J	46,9	1,11	14,5	12,95	0,22	6,93	13,1	1,95	0,11	0,1	2,23	100,1	141
28J	46,6	0,84	15,76	11,28	0,18	9,38	12,18	2,05	0,06	0,07	1,49	99,89	90
29J	45,75	0,85	15,24	11,52	0,18	8,34	11,65	2,17	0,18	0,07	3,66	99,61	173
30J	46,7	1	14,6	12,35	0,2	8,05	12,4	2,07	0,07	0,08	2,43	99,95	99
25J	46,75	1,07	13,95	12,5	0,2	8	12,05	2,33	0,16	0,09	2,19	99,29	117
26J	47,15	1,08	14,75	12,8	0,2	7,14	12,65	2,08	0,09	0,09	1,37	99,4	100
27J	47,4	1,06	14,35	13,06	0,21	7,21	12,7	2,21	0,12	0,09	1,3	99,71	111
21J	45,9	2,02	13,1	16,25	0,23	5,48	10,55	2,68	0,26	0,18	2,9	99,55	162
23J	46,75	1,07	13,9	12,5	0,2	7,82	12,16	2,41	0,14	0,09	2,7	99,74	114
24J	47,05	1,08	14	12,7	0,2	7,64	12,35	2,07	0,19	0,09	2,32	99,69	102

TABLE I

		West dike wall				
		FLOW WEST				
Dike	Site (Fig. 7)	Strike	Plunge	Dynamic	K3	
1J	KILMARIE	156	0	horizontal	9	5
2J	KILMARIE	119	63	upward	10	21
3J	KILMARIE	121	55	upward	22	18
4J	KILMARIE	339	60	down	11	4
5J	ELGOL	undefined				
6J	ELGOL	328	9	down	10	23
8J	ELGOL	294	71	down	9	7
11J	ARDVASAR	undefined				
12J	ARDVASAR	328	27	down	29	2
13J	ARDVASAR	168	16		15	18
14J	ARDVASAR	136	31	upward	33	21
15J	ARDVASAR	69	49	upward	28	26
16J	ARDVASAR	268	61	down	9	8
17J	ARDVASAR	88	34	upward	20	16
18J	TOKAVAIG	326	32	upward	16	4
19J	TOKAVAIG	328	46	down	19	13
20J	TOKAVAIG	266	61	down	5	30
21J	TOKAVAIG	349	38	upward	22	8
22J	DUNVEGAN	288	35	down	27	39
23J	DUNVEGAN	150	48	down	7	20
24J	DUNVEGAN	335	17	down	15	10
26J	ROAG ISLAND	340	62	down	12	18
27J	ROAG ISLAND	328	56	upward	11	13
28J	ROAG ISLAND	322	31	down	23	26

TABLE II

	East dike wall					
	FLOW EAST					
class	Strike	Plunge	Dynamic	K3		class
B	348	40	upward	42	19	B
A	129	17	down	38	22	B
B	130	11	down	11	18	A
NO	315	13	upward	34	25	B
	358	57	down	20	23	A
A	3	39	down	3	18	A
B	317	32	upward	8	27	A
	60	52	down	21	54	A
NO	328	4	down	7	18	A
A	262	84	upward	3	5	A
B	340	36	down	5	26	A
B	104	12	down	10	45	A
B	283	54	upward	29	12	B
B	89	33	down	32	10	B
NO	154	19	downward	12	43	A
B	159	15	down	14	4	NO
A	180	53	down	15	7	B
B	155	5	down	11	16	A
A	134	68	down	10	12	A
A	353	67	upward	21	19	B
B	332	19	down	20	23	A
A	350	20	down	30	30	A
A	354	22	down	19	31	A
A	152	84	down	29	16	B

Dike (both walls)				
		FLOW		
	dike class	Strike	Plunge	Dynamic
41	BB2	341	20	UP
132	AB4			
136	BA4			
130	OB			
		20	23	DOWN
43	AA2	343	25	DOWN
139	BA4			
	OA	60	52	DOWN
	OA	328	16	DOWN
105	AA4			
134	BA4			
133	BA4			
169	BB4			
179	BB4			
	OA	154	19	DOWN
	BO			
45	AB2	217	64	DOWN
45	BA2	341	17	UP
75	AA3	269	71	DOWN
116	AB4			
3	BA1	334	18	DOWN
41	AA2	347	41	DOWN
141	AA4			
65	AB3	321	63	DOWN